Science of the Total Environment 645 (2018) 630–645

Contents lists available at ScienceDirect

Science of the Total Environment

journal homepage: www.elsevier.com/locate/scitotenv

Rainfall isotope variations over the Australian continent – Implications for hydrology and isoscape applications

Suzanne E. Hollins, Catherine E. Hughes *, Jagoda Crawford, Dioni I. Cendón, Karina T. Meredith

Australian Nuclear Science and Technology Organisation, Locked Bag 2001, Kirrawee DC, NSW 2232, Australia

HIGHLIGHTS

- Stable isotopes in precipitation decode the hydrological cycle.
- Long term stable isotopes in Australian precipitation at 15 sites presented.
- Relationships with meteorology/geography used to develop continental isoscape.
- Rainfall isotope and groundwater connections established for NE Australia.

GRAPHICAL ABSTRACT

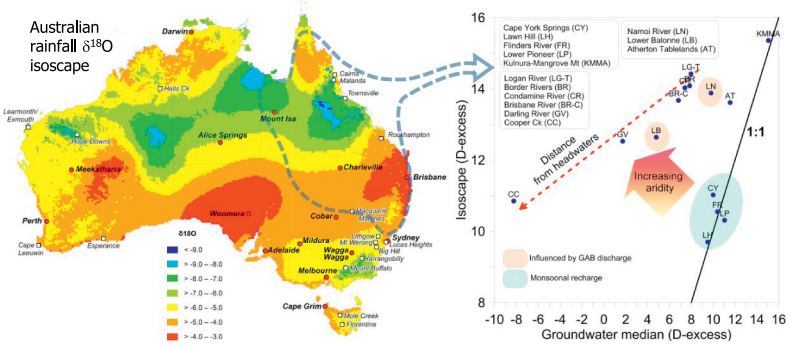

ARTICLE INFO

Article history:
Received 10 April 2018
Received in revised form 12 June 2018
Accepted 6 July 2018
Available online 18 July 2018

Editor: José Virgílio Cruz

Keywords:
Deuterium
Oxygen-18
Precipitation
Local meteoric water line
Groundwater
GNIP

ABSTRACT

This paper presents a continental scale interpretation of δ^2H and $\delta^{18}O$ in Australian precipitation, incorporating historical GNIP data at seven sites (1962–2002) and 8–12 years of new monthly data from 15 sites from 2003 to 2014. The more than doubling of stations and the significant time series duration allow for an improved analysis of Australian precipitation isotopes. Local meteoric water lines were developed for each site, and for the Australian continent. When the annual precipitation weighted values were used, the Australian meteoric water line was $\delta^2H = 8.3\ \delta^{18}O + 14.1‰$.

Precipitation amount was found to be a stronger driver of precipitation isotopes than temperature at most sites, particularly those affected by tropical cyclones and the monsoon. Latitude, elevation and distance from the coast were found to be stronger drivers of spatial variability than temperature or rainfall amount.

Annual isoscapes of δ^2H, $\delta^{18}O$ and deuterium excess were developed, providing an improved tool to estimate precipitation isotope inputs to hydrological systems. Because of the complex climate, weather and oceanic moisture sources affecting Australia, regional groupings were used instead of the climate zone approach and additional data was included to improve the coverage in data poor regions. Regression equations for the isoscape were derived using latitude, altitude and distance from the coast as predictor variables.

We demonstrate how this isoscape can be used as a tool for interpreting groundwater recharge processes using examples from across Queensland and New South Wales, including the Murray Darling Basin. Groundwater isotopes at sites where direct local recharge occurs are similar to rainfall, but for inland sites, which are often arid or semi-arid, a disconnect between shallow groundwater and local rainfall is observed; the departure in deuterium excess for these sites increases with aridity and distance from the headwaters where flooding originates.

* Corresponding author.
E-mail addresses: Suzanne.Hollins@ansto.gov.au (S.E. Hollins), Cath.Hughes@ansto.gov.au (C.E. Hughes), Jagoda.Crawford@ansto.gov.au (J. Crawford), Dioni.Cendon@ansto.gov.au (D.I. Cendón), Karina.Meredith@ansto.gov.au (K.T. Meredith).

https://doi.org/10.1016/j.scitotenv.2018.07.082
0048-9697/

1. Introduction

The stable isotopes of hydrogen (^{2}H, or D) and oxygen (^{18}O) are commonly used as tracers of the hydrological cycle. For example, they can be used in studies of surface water–groundwater interactions (Kalbus et al., 2006), in the estimation of evaporative loss (Skrzypek et al., 2015) and estimating groundwater recharge (Adomako et al., 2010; Cartwright et al., 2017). In addition, the relationship between stable isotopes of precipitation with temperature (and rainfall) has been used to interpret paleoclimate records (Rozanski et al., 1993; McDermott, 2004; Vachon et al., 2010; Treble et al., 2013). In a large number of cases, these relationships have been studied using the Global Network of Isotopes in Precipitation (GNIP) data (e.g. Dansgaard, 1964; Araguás-Araguás et al., 2000). More recently, efforts have been made to predict the spatial variation in isotopic composition (isoscape) of precipitation for regions where little GNIP data exists: the Online Isotopes in Precipitation Calculator (OIPC, Bowen and Wilkinson, 2002; Bowen and Revenaugh, 2003; Bowen, 2018) and the Regionalized Cluster-based Water Isotope Prediction (RCWIP, Terzer et al., 2013). As stated in Terzer et al. (2013), this was due in part to the increasing demand for spatio-temporal predictions of δ^2H and δ^{18}O values in precipitation for use in ecological, wildlife forensics (Bowen et al., 2005) and food source traceability studies after it was found that there was correlation between the δ^2H and δ^{18}O values of some plant, animal and human tissues and isotopic patterns of precipitation.

The isotopic composition of precipitation can be affected by its moisture source, followed by the condensation temperature and the precipitation history in the cloud (Dansgaard, 1964). Further, as the raindrops fall below the cloud, it can be affected by moisture exchange with the surrounding vapour and sub-cloud evaporation, which increases ^{18}O and decreases deuterium excess (defined as $d = \delta^2H - 8 \times \delta^{18}O$; Dansgaard, 1964; Froehlich et al., 2002). Thus the regional climate can have a considerable impact on the isotopic composition of precipitation at a particular site. As a result of these processes, depletion in ^{2}H and ^{18}O occurs with increasing distance from the coast (continental effect) and increasing elevation (altitude effect; e.g. Araguás-Araguás et al., 2000). A latitude effect also exists (Feng et al., 2009), with a local minimum near the equator and two maxima on either side, which coincide with the subtropical highs. These processes can have an impact on the isotopic composition of Australian regional precipitation, as a number of climate zones occur over the Australian continent, with tropical conditions in the north, sub-tropical further south and then temperate conditions in the south of the continent. Moving inland from the coast, we see the vegetation distribution changes from woodlands or rainforest, to grassland regions followed by deserts, reflecting the reduction in rainfall with distance from the coast. Liu et al. (2010), in their study of Australian GNIP data from 1962 to 2002, noted that rainfall at the single inland site in their study was isotopically more depleted than the coastal sites and interpreted this as a continental effect.

The isotopic values of precipitation are also affected by synoptic weather patterns (Barras and Simmonds, 2008; Scholl et al., 2009; Baldini et al., 2010) with some of the lowest ^{2}H and ^{18}O values recorded in rainfall from tropical cyclones (Gedzelman et al., 2003). Tropical cyclones are experienced in the northern half of the Australian continent. Continuous measurements of δ^{18}O and δ^2H in precipitation and water vapour were reported by Munksgaard et al. (2015) during the passage of the tropical cyclone Ita in north-eastern Australia. The Australian monsoon also dominates rainfall in northern Australia. Zwart et al. (2016) undertook a study in northern Australia during two monsoonal events. They found that the size and the activity of the convective envelope played a dominant role in lowering the isotopic composition of precipitation. This was supported by the significant correlation between the isotopic composition of local precipitation and the regional precipitation amount, and also with the integrated precipitation amount of the air mass before arrival at the measurement site.

Inland troughs are also common over the Australian continent, particularly during the warmer months of the year. Frontal systems dominate in the south, predominantly in winter, whilst low-pressure systems are important for coastal regions. Multiple studies investigating the impact of these synoptic weather systems, and of varying moisture sources, on the isotopic composition of precipitation in SE Australia have been undertaken in sites in Tasmania (Treble et al., 2005a; Barras and Simmonds, 2008), Melbourne (Barras and Simmonds, 2009), Adelaide (Guan et al., 2013, 2009), at four sites in the Sydney region (Hughes and Crawford, 2013; Crawford et al., 2013), at the Macquarie Marshes (Crawford et al., 2017), and at the Snowy Mountains (Callow et al., 2014).

Previous interpretations of the spatial characteristics of isotopes in precipitation across the Australian continent by Liu et al. (2010) and Terzer et al. (2013) were based on data from six coastal sites and only one inland site (Alice Springs), as recorded in the Global Network for Isotopes in Precipitation (GNIP) database (IAEA/WMO, 2017). The limited spatial distribution of data available at the time of these studies meant that the range of climatic processes affecting rainfall isotopes across the Australian continent was not fully revealed. This paper builds significantly on these earlier studies, through the presentation and interpretation of much-needed data from an expanded network of rainfall collection sites across the Australian continent, and fills a gap in these important records in the Southern Hemisphere. The expanded rainfall sampling network developed for this study included the recommencement of sampling at all seven of the original Australian GNIP sites, but more importantly included the addition of seven inland continental sites and one further coastal site to improve spatial distribution across the Australian continent (see Fig. 1a and Table 1). Additional data from this study offers improved spatial characterisation of isotopes in rainfall across the Australian continent, as well as extending the GNIP record a further 8–12 years in all stations, enabling characterisation of seasonal trends and the environmental controls on isotopes in Australian rainfall.

This paper also develops and presents the first set of rainfall isoscapes for Australia, allowing for the detailed prediction of the isotopic signature in precipitation at any point on the Australian continent. We demonstrate the predictive capability of these isoscapes and their utility in informing groundwater studies in rainfall isotope data poor regions, through the presentation of a number of case studies of groundwater systems across NE Australia. Understanding the linkage between rainfall and groundwater recharge processes in aquifers containing groundwater with residence times that span several orders of magnitude in timescale is vital for its management and sustainability. This tool will help to better estimate recharge processes and therefore incorporate more realistic predictions in groundwater models.

2. Site description and methods

2.1. Australian climate and weather

Approximately 70% of the Australian continent is classified as arid (desert, average annual rainfall <250 mm) or semi-arid (grasslands, average annual rainfall between 250 and 350 mm) and seven of the fifteen rainfall collection sites in this study fall within these categories (Fig. 1(a), Table 1). These are areas where rainfall is low Fig. 1(b) and unpredictable, with considerable inter-annual variation.

Fig. 1(c–e) shows the typical weather patterns and related air mass distributions that occur across the Australian continent during summer and winter respectively. The monsoonal circulation and the formation of a series of low pressure cells to the north of Australia (Fig. 1(c)) brings very warm, moist and unstable air to the north and north-west of Australia, where it converges across a broad region with tropical continental (Tc) and tropical maritime (Tm) air masses, shown as the intertropical convergence zone (ITCZ) in Fig. 1(d). The rising air along this zone results in extensive convective activity and rainfall - known as the wet

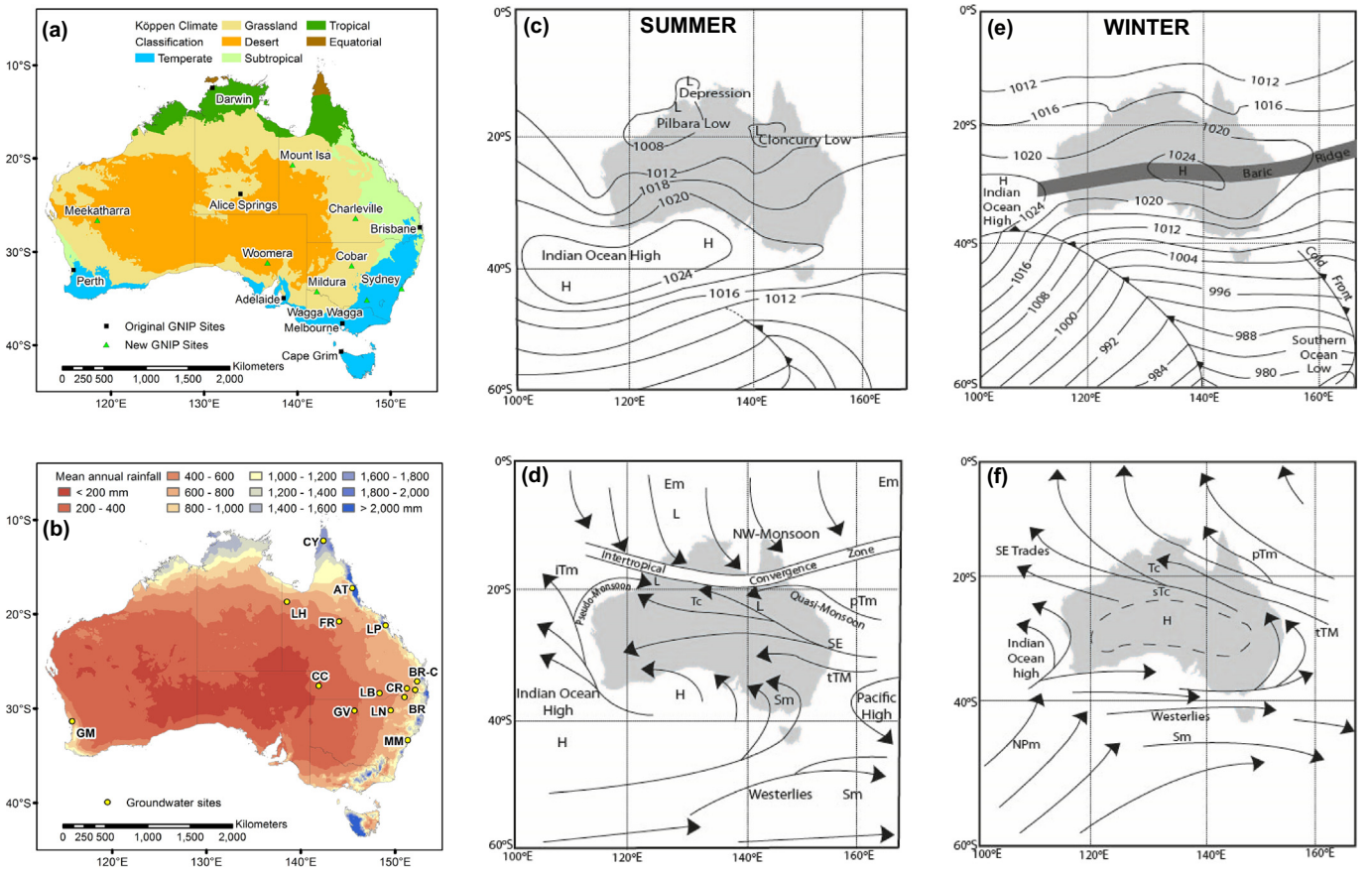

Fig. 1. Australian climate and sampling locations (a) major climate classes based on a modified Köppen classification (Stern et al., 2000). The black squares represent sites for which historical data was available from the GNIP database. The green triangles represent the new sites in the expanded sampling network where no historical rainfall isotope data was available. (b) Annual average rainfall (BOM) and groundwater sites. Typical air-mass distribution (c, e) and weather patterns (d, f) across Australia during summer (February (c, d)) and winter (July (e, f)).
(Source: modified after Sturman and Tapper, 2006).

season. Tropical maritime air flows westward over the central part of the continent, carried onshore by the trade winds. Orographic lifting of this air along the Queensland coast leads to substantial rainfall. As it moves inland it rapidly modifies to become very dry, hot and unstable continental air.

Across southern Australia, as the high pressure systems migrate from west to east, they bring a cycle of hot, dry weather followed by cooler, moister southerly changes. The cold fronts associated with troughs between these highs tend to be weaker in mid-summer.

In winter, the pattern of circulation features changes as the major air masses over Australia move north. The high pressure belt moves north to lie over the cooler centre of Australia, and the highs move slowly from west to east punctuated by cold fronts. A 'baric ridge' links the Pacific and Indian Ocean highs. The westerlies bring cool, moist and cloudy southern maritime (Sm) air to the southern part of the continent. This region is dominated by the occurrence of cold fronts that develop out of the intense low pressure cells in the Southern Ocean (Fig. 1e). Polar air interacts with subtropical air, and a continuous cycle of frontal development is embedded in the prevailing westerly airflow, resulting in substantial precipitation (Sturman and Tapper, 2006). Snow fall in the limited alpine areas occurs when modified polar maritime air (NPm) is drawn from high southern latitudes behind a cold front. In northern Australia, the low pressure cells that were a feature of summer have moved further north along with the ITCZ. The south-east trade winds cover much of the northern region, and the associated stable tropical continental or tropical maritime air masses bringing cooler, drier weather to the area (Fig. 1(f)).

Intense low pressure systems are responsible for many of the severe weather events that result in intense and long duration rainfall along coastal areas of Australia: Tropical cyclones influence the northern parts of the country (mostly in the warmer months); and East Coast Lows occur along the east coast from southern Queensland to Victoria. Large scale remote climate drivers, such as El Niño-Southern Oscillation (ENSO), the Indian Ocean dipole (IOD) and southern annular mode, also have an impact on the rainfall variability over Australia (Risbey et al., 2009).

The rainfall distribution across most of Australia (Fig. 1(b)) is strongly seasonal in character with: a wet summer and dry winter regime in the north (e.g. Darwin, Mt. Isa); a wet summer and relatively dry winter in south-eastern Queensland and north-eastern New South Wales (e.g. Brisbane, Charleville); fairly uniform rainfall in south-eastern Australia (e.g. Sydney, Melbourne, Wagga Wagga, Cobar); a wet winter and dry summer regime in parts of the southern South Australia and south-western Western Australia (e.g. Adelaide, Perth); and low and erratic rainfall throughout much of the western and central inland (e.g. Alice Springs, Mount Isa, Meekatharra, Woomera).

2.2. Sampling sites and history

This paper utilises 8–12 years of new precipitation stable isotope data for 15 Australian sites as well as historical data from seven of these sites available from the GNIP database (IAEA/WMO, 2017) (see Fig. 1(a) and Table 1 – GNIP Site IDs marked with an asterisk). Sample collection for six of the original seven GNIP sites commenced in 1962–

Table 1
Characteristics of the 15 Sampling Sites including the Australian Bureau of Meteorology (BOM) designated Site Name and Number, Data collection period and number data points (n), Latitude (decimal), Longitude (decimal), Elevation (m above sea level), Annual Mean Precipitation, and Annual Mean Surface Air Temperature, Rainfall Climate Class and Modified Köppen Climate Classification (Stern et al., 2000). Site IDs marked with an asterisk (*) include stable isotope data currently available from the GNIP database.

Full BOM Site Name (Site ID)	BOM Site Number	Data collection period	n	Latitude (°N)	Longitude (°E)	Elevation (m asl)	Distance from coast (km)[1]	Precipitation (mm)	Temperature (°C)	Rainfall Climate Class[2]	Modified Köppen climate classification	
Darwin Airport (Darwin*)	14015	1963–1966; 1973–1991; 1995–2014	320	-12.4239	130.8925	30.4	5	1729.3	27.6	Summer Dominant	Equatorial savannah (dry winter)	A T O
Eagle Farm Racecourse* / Brisbane Regional Office* / Brisbane Aero (Brisbane)	40212 / 40214 / 40842	1962–1966; 1973–1982 / 1983–1991 / 1995–2014	466	-27.4304 -27.48 -27.3917	153.0672 153.03 153.1292	7 38 4	10 15 4	1013.5	20.4	Summer	No dry season	SUB-TROPICAL
Perth Airport / Perth CSIRO / Perth Airport (Perth/Perth CSIRO*)	09021 (Perth Airport only)	1962–1966; 1973–1976 / 1983–1986; 1988–2000 / 2005–2014	348	-31.95 -31.95 -31.9275	115.97 115.78 115.9764	15.4 16 15.4	21 3 21	775.1	18.3	Winter dominant	Distinctly dry summer	
Adelaide Airport (Adelaide*)	23034	1962–1967; 1972–1976; 1983–1984; 2005–2014	219	-34.9524	138.5204	2	5	447.0	16.5	Winter	Distinctly dry (and hot) summer	TEMPERATE
Cape Grim BAPS (Cape Grim*)	91245	1985–1991; 1994–95; 1997–2014	274	-40.6828	144.6897	94	1	778.6	13.1	Winter	No dry season (mild summer)	
Melbourne Airport (Melbourne*)	86282	1962–1965; 1968–1969; 1973–1991; 1994–1998; 2005–2014	389	-37.6633	144.8339	113.4	72 (23 to Port Philip Bay)	542.2	14.6	Uniform	No dry season (warm summer)	
Sydney Airport AMO (Sydney)	66037	2006–2014	95	-33.9411	151.1725	6	4	1085.1	17.8	Uniform	No dry season (hot summer)	
Wagga Wagga AMO (Wagga Wagga)	72150	2006–2014	99	-35.1583	147.4573	212	255	574.8	15.6	Uniform	No dry season (hot summer)	
Alice Springs Airport (Alice Springs*)	15590	1962–1970; 1972–1976; 1983–1987; 2005–2014	204	-23.7951	133.889	546	895	284.9	21.0	Arid	Hot (persistently dry)	GRASSLAND
Charleville Aero (Charleville)	44021	2006–2014	83	-26.4139	146.2558	301.6	554	497.7	20.8	Summer	Hot (persistently dry)	
Cobar MO (Cobar)	48027	2006–2014	84	-31.484	145.8294	260	554	402.9	19.0	Uniform	Hot (persistently dry)	
Meekatharra Airport (Meekatharra)	07045	2006–2014	74	-26.6136	118.5372	517	430	236.6	22.4	Arid	Hot (summer drought)	
Mildura Airport (Mildura)	76031	2006–2014	92	-34.2358	142.0867	50	307	292.5	17.1	Winter	Warm (persistently dry)	
Mount Isa Aero (Mount Isa)	29127	2006–2014	62	-20.6778	139.4875	340.3	334	469.8	24.6	Summer Dominant	Hot (winter drought)	
Woomera Aerodrome (Woomera)	16001	2007–2011[3]	46	-31.1558	136.8054	166.6	286 (178 to Spencer Gulf)	185.9	19.2	Arid	Hot (persistently dry)	DESERT

[1]Distance from coast given for current sampling location only.
[2]Summer dominant = marked wet summer and dry winter, Summer = wet summer and low winter rainfall, Uniform = uniform rainfall, Winter = wet winter and low summer rainfall, Winter dominant = marked wet winter and dry summer, Arid = low rainfall.
[3]Four additional samples only from 2006, 2012, 2013.

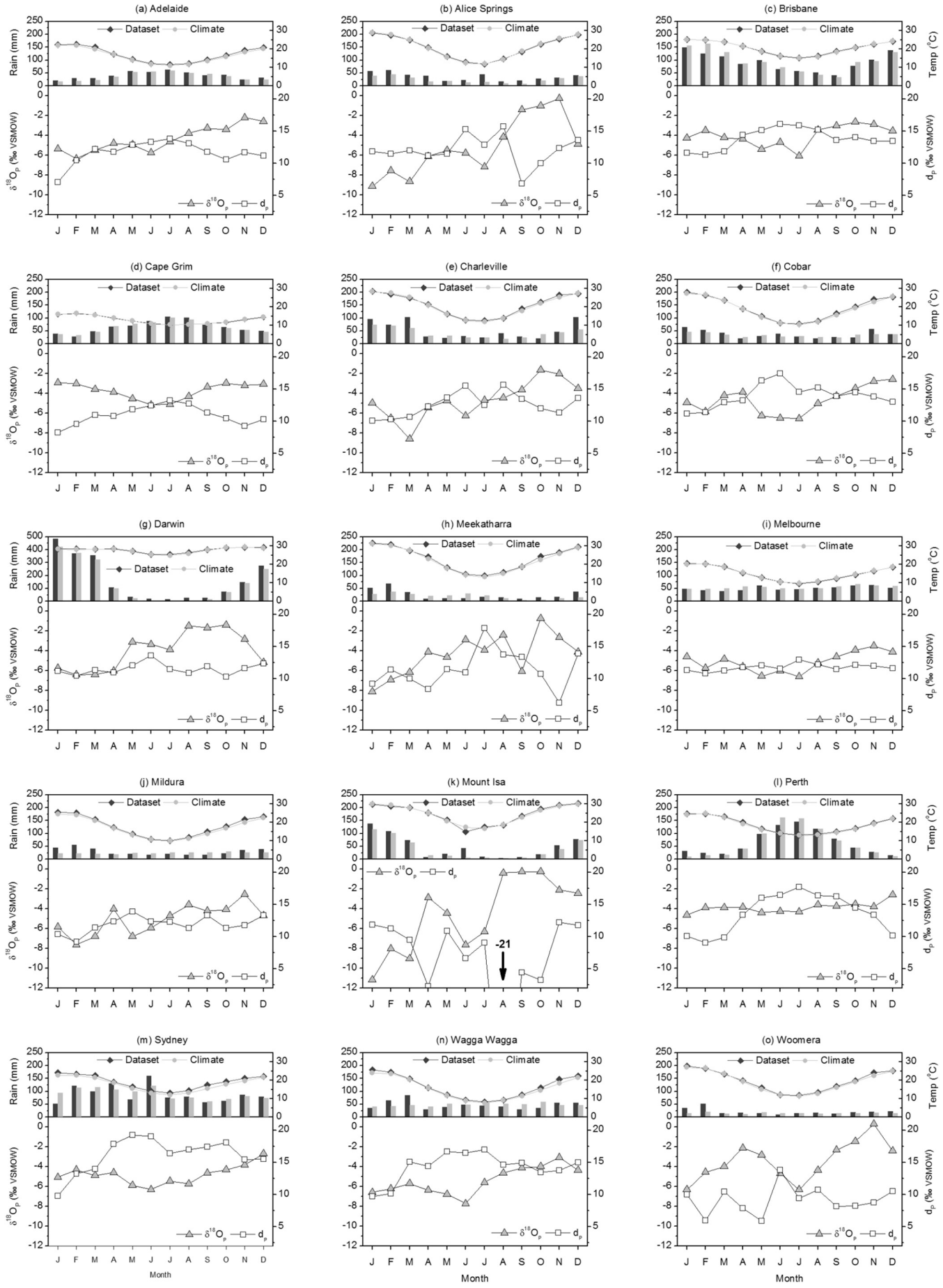
(a) Adelaide
(b) Alice Springs
(c) Brisbane
(d) Cape Grim
(e) Charleville
(f) Cobar
(g) Darwin
(h) Meekatharra
(i) Melbourne
(j) Mildura
(k) Mount Isa
(l) Perth
(m) Sydney
(n) Wagga Wagga
(o) Woomera
Dataset
Climate
Rain (mm)
Temp (°C)
δ18Op (‰ VSMOW)
dp (‰ VSMOW)
δ18Op
dp
J F M A M J J A S O N D
Month
-21

63, with collection commencing in 1979 at Cape Grim. For the purposes of statistics used in this study, stable isotope data from Cape Grim that was collected prior to 1985 has not been used as the corresponding meteorological data (other than precipitation amount) is not available. As can be seen in Table 1, the data collection period was not continuous, with only three sites, of the original seven sites, still being actively sampled by 2005. Data after December 2002 was not available through the GNIP database at the time of writing this paper. Missing stable isotope data for monthly rainfall samples collected from 2003 to 2005, as well as for some samples collected during 2001–2, were obtained directly from the CSIRO Land and Water Isotope Laboratory research team, who had been analysing the rainfall samples since 1982. In 2005, a collaborative arrangement between ANSTO, CSIRO, and the Australian Bureau of Meteorology (BOM) agreed to re-instate sampling at those of the original seven sites which had ceased operating. In 2006, ANSTO instigated an expansion of the Australian rainfall sampling network to a total of 15 sites to include more inland stations (see Fig. 1(a)).

Historical monthly δ^2H and $\delta^{18}O$ data, as well as corresponding monthly temperature, precipitation amount and vapour pressure data for eight of the Australian stations were obtained from the GNIP database (accessible at http://www.iaea.org/water). Meteorological data gaps have been filled, when available, using data from the Australian climate data archive provided by the Australian Bureau of Meteorology Data Service (see Table 1). All rainfall samples from 2005 onwards were collected and analysed as outlined in the following section.

2.3. Sample collection method and analysis

Rainfall samples collected since inception of the IAEA/WMO program in the 1960s were obtained using a composite sampler comprised of a funnel with a rubber bung in a large glass or steel collector. One exception was the Cape Grim site where first an ERNI rainfall collector, and later an EIGENBRODT rainfall collector was used; both had a lid that automatically operated at the onset of rainfall. Whilst the authors cannot be certain of the rainfall sample collection methods for stable isotope analyses prior to 2005, there is no evidence that any technique to prevent evaporation of the sample (e.g. paraffin oil) other than shielding the collection vessel from sunlight and wind was undertaken.

All samples from 2005 onward (except Darwin) were collected as a manual monthly composite of daily rain gauge samples, following the technical procedure recommended for GNIP sampling at http://www-naweb.iaea.org/napc/ih/documents/userupdate/sampling.pdf. This reduces potential evaporative enrichment and vapour exchange compared with the previous technique. However, of the 15 sites Darwin continued to use the previous method. Darwin rainfall is highly seasonal with high monthly rainfall amounts during the monsoon season. This would reduce the impact of evaporative enrichment at this location. A comparison of the weighted and arithmetic averages between the current dataset, and the data from 1962 to 2002 (Liu et al., 2010) shows no systematic differences in *d*-excess that would indicate that evaporation has significantly affected either the historical or recent datasets.

Isotope analyses for samples collected from 2003 to October 2010 were undertaken using Isotope Ratio Mass Spectrometry at the CSIRO Land and Water Isotope Lab (Adelaide) (reported accuracy of ±1.0, ±0.15‰ for δ^2H, $\delta^{18}O$) or Alberta Innovates Technology Futures Isotope Hydrology and Geochemistry Lab (reported accuracy of ±1.0, ±0.2‰ for δ^2H, $\delta^{18}O$). All samples collected from October 2010 onwards were analysed at the ANSTO Environmental Isotope Laboratory using a Cavity Ring-Down Spectroscopy method on a Picarro L2120-I Water Analyser (reported accuracy of ±1.0, ± 0.2‰). All isotope results are reported as per mil (‰) deviations from the international standard, V-SMOW (Vienna Standard Mean Ocean Water). The analytical laboratories for earlier data are listed in the GNIP database.

2.4. Isotopic data quality

The authors have chosen not to "clean up" the isotopic data by following a common method of quality control, which includes removing outliers that lie outside the 2σ or 3σ band of the regression between $\delta^{18}O$ and δ^2H (IAEA, 1992). The data from numerous event based precipitation sampling studies have shown that the variability in isotope values can be large. The "extreme" values identified as lying outside the 3σ band of the regression line may in fact signify real episodes of unusual non-equilibrium conditions that may warrant further investigation of the climate/synoptic conditions producing them. For instance, many of the most depleted values in this dataset result from extreme low pressure events, some of which lie outside the 3σ band because of their abnormally low *d* (e.g. Wagga Wagga, ex Tropical Cyclone Oswald, January 2013; Darwin, Tropical Cyclone Gretel, April 1985). Some authors have also chosen to remove isotope data from low rainfall months (e.g. <2–5 mm/month, Hughes and Crawford, 2013) or with low *d* values (e.g. <3‰, Harvey (2001)) from their statistical treatments, as these samples may have been influenced by evaporation whilst sitting in the collector. However, as many inland sample sites in this study are located in arid and semi-arid areas, the low *d* values observed may in fact be because of sub-cloud evaporation of the rainfall, and not because of sampling errors. We have therefore chosen to include isotope data from all rainfall samples which have been collected, aside from applying a cut-off of precipitation amounts of <2 mm (due to the high frequency of very low *d* values associated with these samples; for example, at Woomera five such samples had a *d* of −7.8‰ or less).

2.5. Meteoric water line methods

Local meteoric water lines (LMWL) were calculated using two regression models: ordinary least squares regression (OLSR) and precipitation amount weighted least squares reduced major axis regression (PWRMA). Precipitation weighted methods for calculating a LMWL reduce the influence of small rainfall events, which have been potentially affected by evaporative enrichment, in the calculation of the slope of the LMWL (Hughes and Crawford, 2012; Crawford et al., 2014) and reduce the need for arbitrary cut-offs. This is most applicable in hydrological studies where these low rainfall events are insignificant in terms of runoff and recharge events, and where it is more appropriate to use a LMWL weighted more towards high rainfall episodes. The details of the OLSR and PWRMA models are outlined in Crawford et al. (2014); PWRMA was chosen because a RMA regression is more appropriate when two variables are related by underlying physical processes as it optimises the fit to both δ^2H and $\delta^{18}O$ (IAEA, 1992).

3. Results and discussion

3.1. Seasonal and spatial variation of the δ^2H, $\delta^{18}O$ and d data

The long-term monthly average temperature and rainfall (calculated on variable length datasets; ranging from 28 years for Cape Grim up to 71 years for Alice Springs) and the corresponding monthly averages for the sampling period are presented in Fig. 2. Average rainfall and

Fig. 2. The seasonal variability of rainfall isotope data (weighted monthly means for $\delta^{18}O$ and corresponding deuterium excess, d_p), rainfall amount (bars) and temperature (diamonds) for the 15 stations currently in operation across Australia. For rainfall and temperature, the monthly averages representing the same monthly intervals for which rainfall samples were collected at a site [dataset] and the long-term monthly climate averages representing all available temperature and rainfall measurements for a site [climate] are shown.

temperature calculated for months with corresponding isotopic data (dataset) generally compare closely to long-term climate averages (climate) indicating that the sampling period is climatically representative. However some notable differences between the monthly rainfall averages for the dataset and long-term climate value do exist, e.g. February at Brisbane; March and December at Charleville; June at Mt. Isa; January, May and June at Sydney; March in Wagga Wagga and February at Woomera. Those months in which the dataset average rainfall was higher than the long-term climate average were mostly associated with the capture within the sampling dataset of extreme events resulting from East Coast Lows, trough systems and residual moisture from low-pressure systems including ex-Tropical Cyclone Yasi (2011). Other months in which the dataset average rainfall amounts were consistently lower than the long-term average may reflect an absence of infrequent extreme events during the sampling period. Supplementary Fig. S1 also gives an indication of how climatically representative the sampling period in this study was. Fig. S1 shows the total accumulated precipitation sampled for each month at each site and the corresponding interquartile range of $\delta^{18}O$ values. In general, the range in monthly isotopic values is greater than the range for the inland sites. The variability in isotopic mean/median between months is generally greater for those sites with a smaller number of data points indicating that a longer dataset may be required to consider the statistical monthly variation.

Fig. 2 illustrates the seasonal patterns in the stable isotopes ratios δ^2H, $\delta^{18}O$ in Australian precipitation. A weak seasonal variation in the isotopic composition is observed with winter minimum and spring-summer maximum in the coastal temperate sites of Adelaide, Brisbane, Cape Grim, Melbourne and Sydney. Inland sites (Alice Springs, Charleville, Cobar, Mildura, Mt. Isa, Wagga Wagga, and Woomera) commonly exhibit a spring maximum and lower values in summer and winter. A spring maximum was also found for four sites in the Sydney Basin (Hughes and Crawford, 2013) which was attributed to (1) smaller precipitation amounts in spring, and sub-cloud evaporation; and (2) first-stage rainout. Both of these processes result in more isotopically enriched rainfall and would be considered valid for the inland sites in this study. These sites generally experience dry winters and the humidity tends to be lower in winter to spring which would also increase sub-cloud evaporation. Darwin, which is subject to monsoonal rain, has a bimodal distribution with low values during the wet season from December to April and high values during the dry season. Feng et al. (2009) found a local isotopic minimum near the equator which coincides with the movement of the Intertropical Convergence Zone (ITCZ), also identified by Matsui et al. (1983) at Belém (Brazil) and Edirisinghe et al. (2017) in Sri Lanka. We see strong evidence for this not only in Darwin but in other northern Australian sites, such as Mount Isa and Alice Springs, which are influenced by the monsoon. In mid-summer the southward shift in the ITCZ, which results from the convergence of equatorial maritime with tropical continental and tropical maritime air, causes air to rise producing significant precipitation over northern Australia (Sturman and Tapper, 2006).

As expected, the d is higher in the austral winter months (June–August) than in the summer months (December–February) for all sites except Mt. Isa, where the winter record is dominated by a single depleted extreme event in June 2007 which accounts for 75% of all winter rainfall sampled in this study. Isotopically enriched rainfall with low d was recorded at Mt. Isa in August to October, which corresponds to small rainfall events, suggesting re-evaporation of raindrops below the cloud. The higher d at other sites in winter may be attributed to cold air masses with low relative humidity travelling over the ocean, thus resulting in higher kinetic fractionation during evaporation at the moisture source (Liotta et al., 2006; Pfahl and Sodemann, 2014). Comparing weighted averages for all samples with those with precipitation ≥5 mm it can be noted that whilst the subset with the small rainfall amounts removed has a marginally more depleted average, this difference is negligible for the coastal sites and below the reported analytical error for the inland sites, and the difference in d is always <0.2‰.

Larger d values were seen in Sydney, Wagga Wagga, Cobar and Perth in particular. To examine if this was as the result of the shorter time series for these sites, precipitation weighted values for the shorter periods (i.e. for years 2007–2014) were also calculated for the long-term sites (Supplementary Table S1). A higher d resulted for the years from 2007 for a number of the long term sites, e.g. in Brisbane, but excluding Perth, when using the entire data set the precipitation weighted d_p was 13.5‰, whereas when using data from 2007 onwards the d_p was 14.2‰ (comparable to Wagga Wagga), highlighting the value of longer time series. Carrying out a trend analysis found a slight increasing trend in $\delta^{18}O$ over the period of record at Brisbane (0.0075‰ per year) and Adelaide (0.008‰ per year) and also in d at Brisbane (0.01‰ per year) but no significant trends at the other sites. Other than Darwin and Melbourne the long term precipitation weighted average values of $\delta^{18}O$ and δ^2H are more enriched in the current longer data set than that in Liu et al. (2010). In particular, the 2007–2014 period had significantly more depleted precipitation at Darwin because the historical dataset had a number of very large (>700 mm/month) rainfall events that were more enriched than the general precipitation amount effect would predict. Brisbane also exhibits a difference with a reduction in the amount of depleted rainfall months in the 2007–2014 period.

Annual, seasonal and monthly arithmetic and weighted average values of δ^2H, $\delta^{18}O$ and d are listed in Supplementary Table S1 and the monthly data plotted in Supplementary Fig. S2. The weighted means for all sites across the Australian continent are more depleted than the arithmetic mean, reflecting the seasonality in rainfall amounts and isotopic values. In addition, the weighted mean d_p values are higher than the arithmetic mean d values for inland sites in particular, suggesting that sub-cloud evaporation is important. Guan et al. (2013) found that where sub-cloud processes have an impact, the precipitation-weighted mean is lower than the arithmetic mean and the precipitation weighted d_p value is higher than the arithmetic mean. This is seen at most sites and is particularly evident at the arid inland site, Alice Springs (Supplementary Table S1 and Fig. S2).

The most isotopically depleted monthly rainfall samples in the entire dataset occurred at Mount Isa. In order to understand processes leading to this depletion, back trajectories using HYSPLIT (Draxler and Rolph, 2003) were generated for some of the months with the most isotopically depleted precipitation. In these cases it was found that substantial precipitation had occurred prior to the sampling site (using the HYSPLIT generated precipitation amount at each back trajectory location before the sampling site), thus indicating isotopic depletion due to the prior rainout. Heavy and prolonged rainfall occasionally falls at Mount Isa with the passage of ex-tropical cyclones (e.g. cyclone Ellie January–February 2009, for which ^{18}O depleted rainfall was sampled). The mean stable isotope ratios of rainfall from tropical cyclones were found by Lawrence and Gedzelman (1996) to be distinctly lower than those of other tropical and summer rainfall events, which can be attributed to the high condensation efficiency of tropical cyclones and storms. This has a definite effect on precipitation at both Darwin and Mount Isa, and is occasionally seen at other sites such as Brisbane, Charleville and Meekatharra, and further south. The isotopic evolution of precipitation from tropical cyclone Ita (April 2014; Trinity Beach P = 231 mm, $\delta^{18}O = -10.2$‰), in north-eastern Australia, has been detailed in Munksgaard et al. (2015) and isotopic values associated with cyclones in north-west Australia are also reported to be significantly depleted (Skrzypek et al., 2018). However, whilst some of the most depleted rainfall in this dataset is due to tropical cyclones and low-pressure systems, not all of these events result in depleted rainfall. The weighted average composition for 15 individual months when tropical cyclones affected Darwin was more depleted (precipitation weighted average δ^2H of −40.9 and $\delta^{18}O$ of −6.4) than the average of all data, however, five of those months

were more enriched than the average. This is most likely due to the observed behaviour of the isotopic composition of precipitation from cyclones, which is variable depending on the distance from the eye of the cyclone (e.g. Munksgaard et al., 2015).

3.2. Local meteoric water lines

The relationship between $\delta^{18}O$ and $\delta^{2}H$, known as the meteoric water line, provides a useful frame of reference for comparing different sites and regions, as well as for hydrological and groundwater studies where rainfall is a significant end member. Both ordinary least squares (OLSR) and precipitation weighted reduced major axis (PWRMA) regression models (Crawford et al., 2014) were used to determine Local Meteoric Water Lines (LMWL) for the Australian sites using all available monthly data from the 15 stations (Fig. 3; Supplementary Table S2). There is a significant increase in the slope and intercept of the LMWL calculated using PWRMA relative to that of the OLSR. This reflects the removal of a bias in the calculation of the LMWL towards the small rainfall events which may have experienced secondary evaporation effects during rainout, resulting in lower *d* and more enriched isotopic values. These events occur most frequently in the arid and semi-arid interior of Australia (e.g. Macquarie Marshes, NW-NSW; Crawford et al., 2017; where the PWRMA slope was 7.2, still lower than the slope of 8 for the Global MWL) where higher temperatures and low humidity are experienced for much of the year, as well as the Mediterranean climate zones in South and Western Australia which experience hot dry summers (Hughes and Crawford, 2012). Nine of the fifteen sites in this study lie in these zones.

In order to compare seasonal variations, the LMWLs were also determined using both regression methods for the summer (DJF) and winter months (JJA). Generally, the slopes are greater in winter for the southern coastal and inland sites and greater in summer for the northern and eastern coastal sites, broadly reflecting the seasonal rainfall dominance. However, it also observed that there was a group of sites with significantly less difference between summer and winter that appeared to correlate with shorter datasets used to calculate the LMWLs. We initially considered that this may be a statistical artefact whereby extreme rainfall events may bias the calculations for the relatively short seasonal datasets (e.g. Mount Isa and Woomera had data from only 6 and 8 winter samples, respectively). To test this theory, LMWLs were developed for Melbourne and Perth using only data from the time period corresponding to the more recent sites (i.e. 2006–2014). It was found that the differences in the slopes of these seasonal LMWLs for these abridged datasets did not increase, and therefore we do not believe the observed differences were due to statistical artefacts. As most of the sites with longer datasets are located on the coast, we also considered the possibility that there may be a moderation in the difference between seasonal LMWLs due to the close proximity of the sites to the dominant moisture source for the rainfall. However, this is unlikely as a significant difference was also observed at Sydney, which is also located on the coast. Hence, we consider that the variability between the seasonal LMWLs is not simply attributable to a seasonal effect or geographical location, but is also due to other processes such as the different weather systems contributing to rainfall at each of the sample sites and below cloud evaporation in hot and dry locations. For example, the smaller slope of the LMWL observed at Alice Springs in summer, could be attributed to below cloud evaporation (e.g. Harvey and Welker, 2000). The larger slope in the observed LMWL at Darwin during the summer season is consistent with other sites affected by monsoonal rainfall (e.g. Kumar et al., 2010).

The use of our measured monthly rainfall data to construct an Australian MWL could be of considerable value for use in comparing rainfall isotopic data in Australia with other continents, regions or islands, or as a frame of reference for other Australian precipitation data. However, the weighting of the stations to construct such a MWL needs to be carefully considered because the distribution of our study sites does not fully represent the range of climate and geography in Australia, and there are large differences in rainfall amount between sites. The use of precipitation weighted regressions, in this case, has the potential to introduce an undesirable bias towards high rainfall coastal sites and extreme events which may not reflect the precipitation over the majority of the inland areas of the continent (Crawford et al., 2014). Use of all available monthly data could exacerbate this because it is mainly the coastal sites that have long data records and a larger number of samples per year than the drier inland sites. An Australian rainfall isoscape was also developed in this study (Section 3.3.5) in order to estimate the spatial distribution of isotope values for regions where no sample data is available. The gridded precipitation $\delta^{18}O$ and $\delta^{2}H$ values which were predicted through the development of this isoscape can also be used to develop a national MWL – the advantage of this approach is that it can result in a more geographically (non-weighted) or hydrologically (precipitation weighted) representative MWL for the entire country or any sub- region.

Using the isoscape gridded precipitation data, the non-weighted RMA derived Australian MWL was calculated to be $\delta^{2}H = 8.6\delta^{18}O + 14.4$ and the precipitation weighted RMA MWL was $\delta^{2}H = 8.6\delta^{18}O + 15.3$. As indicated above, we recommend the use of these MWLs as most representative for the Australian continent. For comparison, we also present Australian MWLs calculated using the available sample data: (1) a non-weighted RMA regression on the weighted average annual values for all 15 sites (calculated from monthly samples,) gives a MWL of $\delta^{2}H = 8.3\delta^{18}O + 14.1$, (2) a precipitation weighted RMA regression on all measured monthly rainfall data ($n = 2855$) gives a MWL of $\delta^{2}H = 7.9\delta^{18}O + 12.3$, and (3), RMA regression on precipitation weighted monthly average values gives a MWL of $\delta^{2}H = 7.2\delta^{18}O + 7.6$ (parameters for all regressions are given in Supplementary Table S2). The difference between each of these calculated MWLs is significant, and highlights the need to take care in the development of regional MWLs from a spatially irregular sampling network.

3.3. Environmental controls on stable isotopes in Australian rainfall

3.3.1. Temperature effect

As decreasing temperature drives the rainout process, a strong correlation between temperature and isotopes in precipitation should occur, i.e. where a temperature gradient exists, there will be a gradient in the $\delta^{18}O$ and $\delta^{2}H$ signatures. Dansgaard (1964) identified a global linear relationship between surface air temperatures and mean annual $\delta^{18}O$ in precipitation as

$$\delta^{18}O = 0.695T_{annual} - 13.6‰$$

However, at the regional to local scale, the T-$\delta^{18}O$ relationship may not hold true because of the dominance of continental or rainout effects, the impact of sub-cloud evaporation, the seasonality of rainfall or physiographic variations (Clark and Fritz, 1997). When the T-$\delta^{18}O$ relationship for each of the individual sample locations is calculated, the slopes are all positive but much lower than the above global slope. The r^2 values are also generally low, when either the monthly sampled data is used or annual average values are used in the calculations (Supplementary Table S3). For the Australian continent, the linear relationship between mean surface air temperature and mean annual $\delta^{18}O$ in precipitation ($r^2 = 0.23$) is

$$\delta^{18}O = -0.115T_{annual} - 2.65‰$$

The slope of this relationship is influenced by the continental effect and the fact that different processes dominate at the different sites, e.g. at Alice Springs, Mt. Isa and Darwin, the amount effect has a higher r^2 value than the temperature effect (Supplementary Table S3; discussed in the next section).

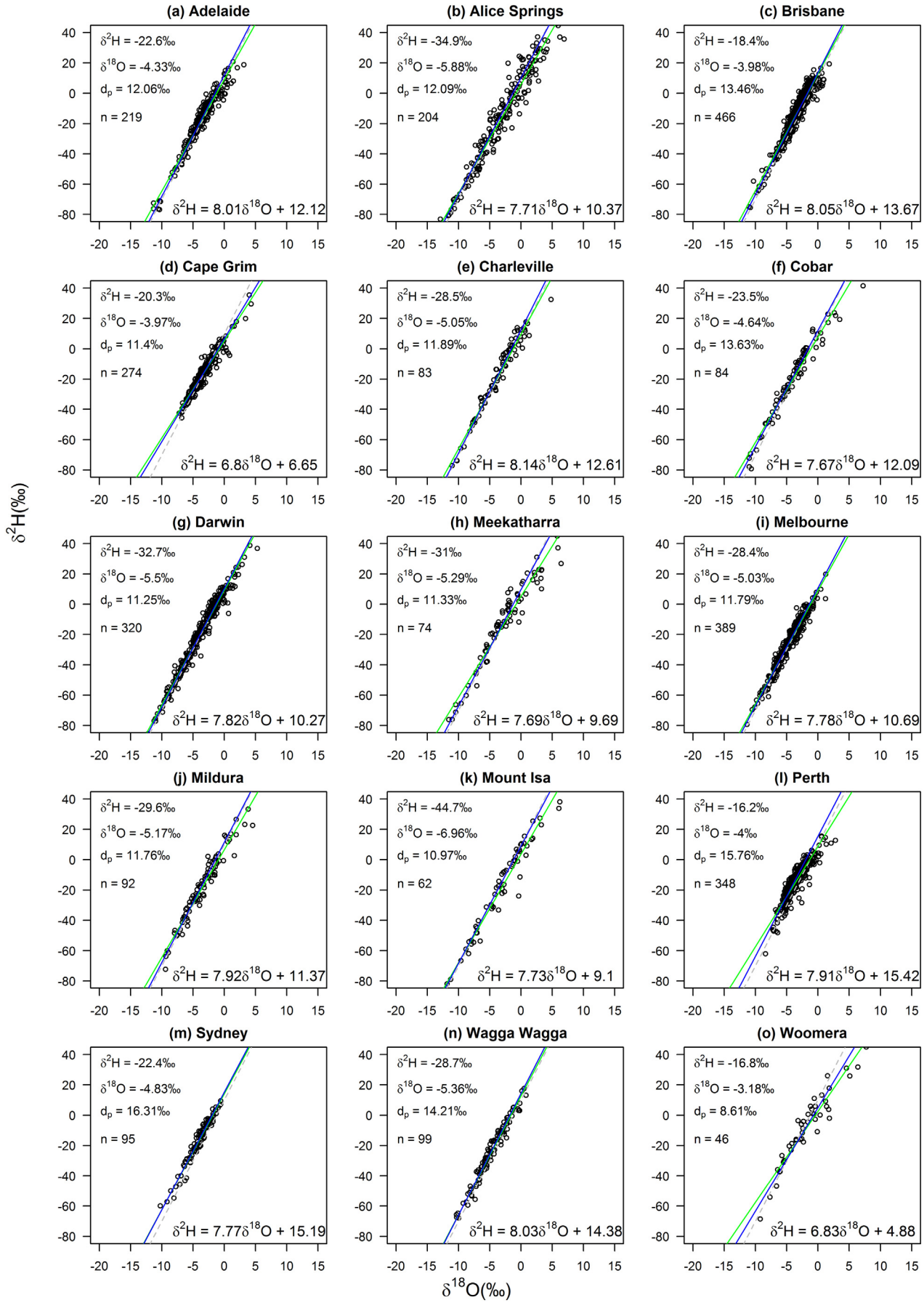
(a) Adelaide
δ²H = -22.6‰
δ¹⁸O = -4.33‰
dp = 12.06‰
n = 219
δ²H = 8.01δ¹⁸O + 12.12
(b) Alice Springs
δ²H = -34.9‰
δ¹⁸O = -5.88‰
dp = 12.09‰
n = 204
δ²H = 7.71δ¹⁸O + 10.37
(c) Brisbane
δ²H = -18.4‰
δ¹⁸O = -3.98‰
dp = 13.46‰
n = 466
δ²H = 8.05δ¹⁸O + 13.67
(d) Cape Grim
δ²H = -20.3‰
δ¹⁸O = -3.97‰
dp = 11.4‰
n = 274
δ²H = 6.8δ¹⁸O + 6.65
(e) Charleville
δ²H = -28.5‰
δ¹⁸O = -5.05‰
dp = 11.89‰
n = 83
δ²H = 8.14δ¹⁸O + 12.61
(f) Cobar
δ²H = -23.5‰
δ¹⁸O = -4.64‰
dp = 13.63‰
n = 84
δ²H = 7.67δ¹⁸O + 12.09
(g) Darwin
δ²H = -32.7‰
δ¹⁸O = -5.5‰
dp = 11.25‰
n = 320
δ²H = 7.82δ¹⁸O + 10.27
(h) Meekatharra
δ²H = -31‰
δ¹⁸O = -5.29‰
dp = 11.33‰
n = 74
δ²H = 7.69δ¹⁸O + 9.69
(i) Melbourne
δ²H = -28.4‰
δ¹⁸O = -5.03‰
dp = 11.79‰
n = 389
δ²H = 7.78δ¹⁸O + 10.69
(j) Mildura
δ²H = -29.6‰
δ¹⁸O = -5.17‰
dp = 11.76‰
n = 92
δ²H = 7.92δ¹⁸O + 11.37
(k) Mount Isa
δ²H = -44.7‰
δ¹⁸O = -6.96‰
dp = 10.97‰
n = 62
δ²H = 7.73δ¹⁸O + 9.1
(l) Perth
δ²H = -16.2‰
δ¹⁸O = -4‰
dp = 15.76‰
n = 348
δ²H = 7.91δ¹⁸O + 15.42
(m) Sydney
δ²H = -22.4‰
δ¹⁸O = -4.83‰
dp = 16.31‰
n = 95
δ²H = 7.77δ¹⁸O + 15.19
(n) Wagga Wagga
δ²H = -28.7‰
δ¹⁸O = -5.36‰
dp = 14.21‰
n = 99
δ²H = 8.03δ¹⁸O + 14.38
(o) Woomera
δ²H = -16.8‰
δ¹⁸O = -3.18‰
dp = 8.61‰
n = 46
δ²H = 6.83δ¹⁸O + 4.88
δ²H(‰)
δ¹⁸O(‰)

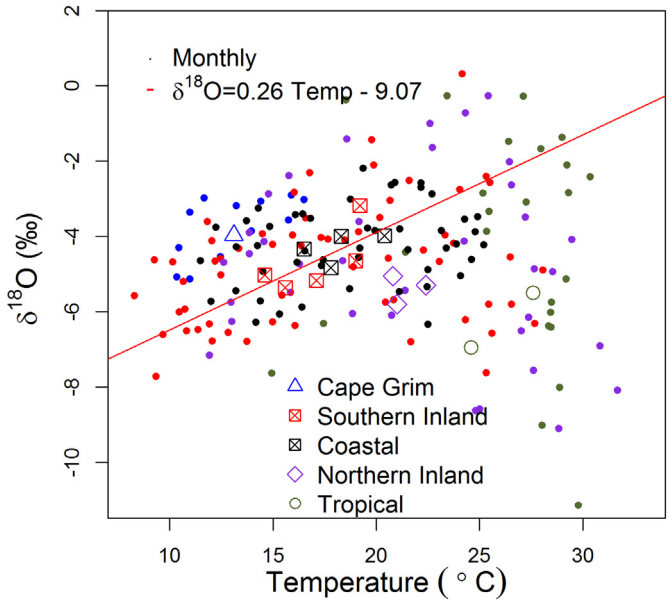

Fig. 4. Amount weighted monthly and annual mean $\delta^{18}O$ versus mean air surface temperature. Groupings are: Southern Inland (Melbourne, Wagga Wagga, Cobar, Mildura and Woomera), Coastal (Adelaide, Sydney, Brisbane and Perth), Northern Inland (Alice Springs, Charleville and Meekatharra), Tropical (Darwin and Mount Isa). Individual monthly data for the sites in each group are represented by dots of the same colour.

On closer examination of the annual mean (temperature, $\delta^{18}O$) relationship in Fig. 4 we see three main groups, from left to right: (1) an enriched value at the lowest temperature (Cape Grim, which is located the furthest south and receives first stage rainout from frontal systems passing across the Southern Ocean); (2) a group of values (southern inland and coastal sites) in which a positive relationship between $\delta^{18}O$ and temperature exists; (3) followed by a group of values with almost very little change in $\delta^{18}O$ with temperature, which consists of the tropical sites (Darwin and Mt. Isa, for which isotopes are depleted due to the amount effect) as well as the northern inland sites of Charleville, Alice Springs and Meekatharra, for which there is depletion due to the continental effect. If the first and last sets are removed a better relationship exists between temperature and $\delta^{18}O$ for the southern inland and coastal sites, with a regression line of $\delta^{18}O = 0.259\,T - 9.07‰$, and an r^2 of 0.47.

3.3.2. Precipitation amount effect

The initial liquid phase of rainfall is enriched in the heavy isotopes when compared to rainfall later in the rain event. As a consequence, the rainfall becomes more depleted (lighter) in heavy isotopes as the rain continues to fall, and this is known as the "amount effect" or "rainout effect" (Dansgaard, 1964). Risi et al. (2008) identify two processes that explain the "amount effect" in convective systems, in the tropics: the re-evaporation of falling rain and diffusive exchange with surrounding vapour; and the recycling of the sub-cloud layer feeding the convective system.

A negative slope is seen between $\delta^{18}O$ and precipitation amount at all sites with a higher r^2 value than that of local surface temperature (Supplementary Table S3). In particular, the correlation is significant for Sydney, Alice Springs, Mildura, Mt. Isa and Darwin. Dansgaard (1964) found that this effect is seen throughout the year in most tropical stations and in the summer at mid-latitudes. This is supported by our findings of a stronger correlation between $\delta^{18}O$ and precipitation in summer at a large number of the sites.

The partial correlation coefficients presented in Supplementary Table S3 are an indication of the covariance between the monthly rainfall $\delta^{18}O$ values and the monthly rainfall amount (P; when the effect of temperature has been removed) and average monthly surface air temperature (T, when the effect of rainfall amount has been removed). There is little difference between the correlation coefficients between the raw and deseasonalised data, which indicates that the seasonality of temperature and rainfall have little effect on the isotopic composition. The exception is the northern-most sites affected by tropical cyclones and the monsoon (Darwin, Mt. Isa, Meekatharra) which do show a lower correlation for precipitation when temperature effects are removed.

3.3.3. Relationship of $\delta^{18}O$ with vapour pressure (e_a) and relative humidity (RH)

The relative humidity at a site has an impact on the sub-cloud evaporation which results in isotopically more enriched remaining precipitation (Dansgaard, 1964). We see a negative relationship between relative humidity and precipitation $\delta^{18}O$ values consistent with this, particularly for the inland sites, where the RH-$\delta^{18}O$ correlation was generally better than that for temperature or precipitation (Supplementary Table S3). For the relationship between $\delta^{18}O$ and vapour pressure the best r^2 values were those for Mount Isa and Alice Springs. This correlation was negative, implying that isotopically more depleted $\delta^{18}O$ values were seen under higher vapour pressure; however, the correlation for the other sites was low.

3.3.4. Latitude, altitude and continental effects

A broad latitudinal gradient is observed across the continent (Fig. 5 (a)), with a general trend for increasing enrichment poleward ($\delta^{18}O = -0.066 \times \text{latitude} - 6.84$), rather than the opposite observed in the global data-set for mid-latitudes (e.g. Rozanski et al., 1993). The observed pattern is similar to that presented by Feng et al. (2009; where a positive trend in $\delta^{18}O$ was seen from the equator to about 30° north and south and then a rapid decrease was observed) and reflects the dominance of the monsoonal (Zwart et al., 2016) and tropical cyclone regimes (Munksgaard et al., 2015; Skrzypek et al., 2018) to the north and the diverse weather types and oceanic moisture sources impacting the southern half of the continent.

The altitude range of the sites is small, with the lowest altitude of 2 m asl and the highest at 546 m asl. Even so, a trend is seen in the $\delta^{18}O$ values, with more depleted values at the higher altitudes ($\delta^{18}O = -0.0026$ altitude $-4.4‰$; r^2 of 0.28; Fig. 5(b)), whereas there is no clear trend in *d*. An altitude effect is reported by Callow et al. (2014) and Tadros et al. (2016) for the Snowy Mountains (950–2045 m asl), and Hughes and Crawford (2013) for the Sydney Basin (152–1178 m asl), with precipitation more depleted than the corresponding lowland sites from this network (Wagga Wagga and Sydney). This indicates that the expanded GNIP network is less effective for defining the isotopic composition of rainfall along the Great Dividing Range along the east coast of Australia than it is for coastal and inland Australia. This is explained further in Section 3.3.5 where the Australian isoscapes are developed and discussed.

Land masses force rainout from vapour masses as they move inland, so that the residual vapour and subsequent rainfall at the centre of a

Fig. 3. Local meteoric water lines for each of the fifteen collection sites, calculated using all data (circles). The dashed line represents the GMWL ($\delta^2H = 8{\cdot}\delta^{18}O + 10$; Craig, 1961), and the LMWLs are shown in blue (precipitation weighted reduced major axis regression, PWRMA, equation in bottom right hand corner) and green (ordinary least squares regression, OLSR). Parameters for these LMWLs are listed in Supplementary Table S2. The precipitation weighted d_p, $\delta^{18}O$, δ^2H, and sample number n are shown in top left hand corner (Supplementary Table S1).

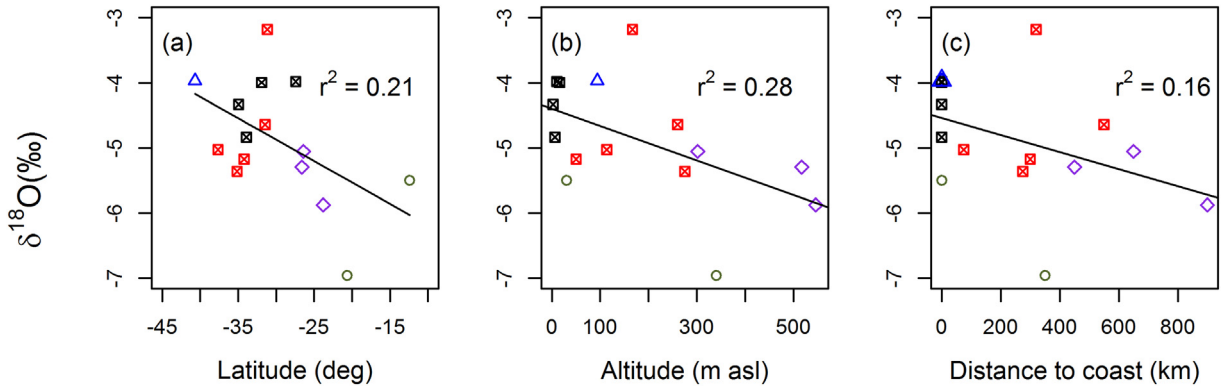

Fig. 5. The distribution of the weighted annual $\delta^{18}O$ values in precipitation with (a) latitude (p-value = 0.05), (b) altitude (p-value = 0.04), and (c) distance from the coast (p-value = 0.13).

large land mass or continent, such as Australia, becomes progressively more depleted in heavy isotopes – the "continental effect". However, this effect may be counteracted by the contribution of isotopically enriched recycled continental moisture back into the atmosphere from evaporated soil and surface water. Furthermore, sub-cloud evaporation also leads to isotopically more enriched precipitation, which can also counter-act the continental effect; however, this has a lower impact during large rainfall events. To examine if a continental effect exists for the isotopic composition of Australian precipitation a linear regression was undertaken for the $\delta^{18}O$ with distance from the coast (Table 1).

The resulting regression line was $\delta^{18}O = -0.0011 \times \text{distance} - 4.54‰$, with an r^2 value of 0.16 (Fig. 5(c)). The correlation is low, which may be because there are a range of climatic zones across the continent. Not all sites receive the majority of their rainfall along a trajectory perpendicular to the coast and many sites, particularly in Eastern Australia, receive significant rainfall from the nearest coastline as well as along continental trajectories 1000 km to the west. Along a transect from Adelaide-Mildura-Wagga Wagga we see depletion (presumably due to rainout), with precipitation weighted $\delta^{18}O$ values of −4.35, −5.22 and −5.39‰, respectively. Undertaking a regression fit of $\delta^{18}O$ with distance from Adelaide resulted in a regression line of $\delta^{18}O = -0.0032 \times \text{distance} - 4.34‰$, which is very close to the regression based on all data, but with a much improved r^2 value of 0.9 due to the removal of variability due to other factors (such as varying moisture sources and trajectories).

3.3.5. Development of an Australian isoscape

Interpolation of a sparse spatial dataset such as presented in this paper is difficult. Simple interpolation methods such as kriging cannot account for the climatic and geographic factors that influence precipitation isotope composition. Interpolation prediction models incorporating first latitude and altitude (Bowen and Wilkinson, 2002), distance from the coast (Bowen and Revenaugh, 2003), then adding meteorological variables (e.g. Lykoudis and Argiriou, 2007) and, most recently, climatic zones (Terzer et al., 2013) are believed to be an improvement on simple interpolation.

The Regionalised Cluster-Based Water Isotope Prediction (RCWIP) gridded precipitation $\delta^{18}O$ and $\delta^{2}H$ (Terzer et al., 2013; IAEA, 2014) overestimates both $\delta^{18}O$ and $\delta^{2}H$ for most months at the 15 sites in this dataset, except for Cape Grim. The correlation between gridded outputs and annual weighted averages was moderate to strong for the coastal sites with r^2 ranging from 0.41 to 0.80 (Supplementary Table S4), with the exception of Perth and most of the inland sites. Generally, RCWIP predicts the winter $\delta^{18}O$ and $\delta^{2}H$ well at most Australian sites, but performs very poorly in summer, when it overestimates both $\delta^{18}O$ and $\delta^{2}H$ by more than the interpolation uncertainty for many months at all sites (excluding Cape Grim, where it is underestimated) and up to ~11.8‰ for $\delta^{18}O$ and 92‰ for $\delta^{2}H$ for January. RCWIP uniformly predicts a winter minimum and summer maximum, whereas most Australian sites have their most enriched rainfall in spring-early summer and many have their most depleted rainfall in late summer-autumn. In zones with winter dominant or uniform rainfall distribution, a reasonable annual weighted average match is seen despite RCWIP's inability to match the observed isotopic seasonality. Where the rainfall climate is arid or summer dominated RCWIP performs more poorly and in the northern half of Australia, there may be an improvement to be made by having additional sites to define the regression parameters for this climate zone. To achieve this we used additional rainfall isotope data from sites shown in Fig. 6a (Cartwright and Morgenstern, 2016; Cook et al., 2001; Crawford et al., 2017; Crosbie et al., 2012; Goede et al., 1982, 1986, 1990; Hughes and Crawford, 2013; Munksgaard and Zwart, 2017; Tadros et al., 2016; Treble et al., 2005b; Skrzypek et al., 2018; Stephen Lewis, James Cook University, pers. comm 17 June 2015; Supplementary Table S5b).

To generate isoscapes we used relationships across the continent between geographic parameters and the precipitation weighted average $\delta^{18}O$, $\delta^{2}H$ and d_p values from each site. Aside from using the geographic variables as predictors for isotopic composition, we investigated if long-term average precipitation, temperature, relative humidity and vapour pressure at the sites could also be used as predictor variables in the development of an isoscape. We found that relative humidity, vapour pressure and precipitation amount were poor predictors of rainfall isotopes on a continental basis. A significant correlation was found when temperature was used, by itself; however, when latitude and altitude were also included in the regression the marginal contribution of temperature was low, hence temperature was not used in the isoscape development.

Due to the large number of climatic zones and moisture sources over the Australian continent and the small number of sampling sites for a number of these climatic types, we were unable to generate an isoscape using the method presented by Terzer et al. (2013). However, by grouping the available sites into four coastal regions (east, west, south and north) and an inland group (Supplementary Table S5) we were able to obtain regression relationships of $\delta^{18}O$ with a combination of predictor variables; latitude, altitude and distance from the coast. The regression equations had the following form (following from Bowen and Revenaugh, 2003, with the addition of distance from the coast):

$$y = a(Lat)^2 + b|Lat| + cAlt + dDistance \quad (1)$$

where y was $\delta^{18}O$, $\delta^{2}H$ or d_p and *Distance* was the distance from the nearest coast. For the north, west and south sites, latitude, altitude and distance from the coast were used. For the east and inland groups only latitude and altitude were used. For the east sites, the distance from the coast was not significant and did not increase the r^2 of the fit. Whereas, only five sites were available for the inland group and

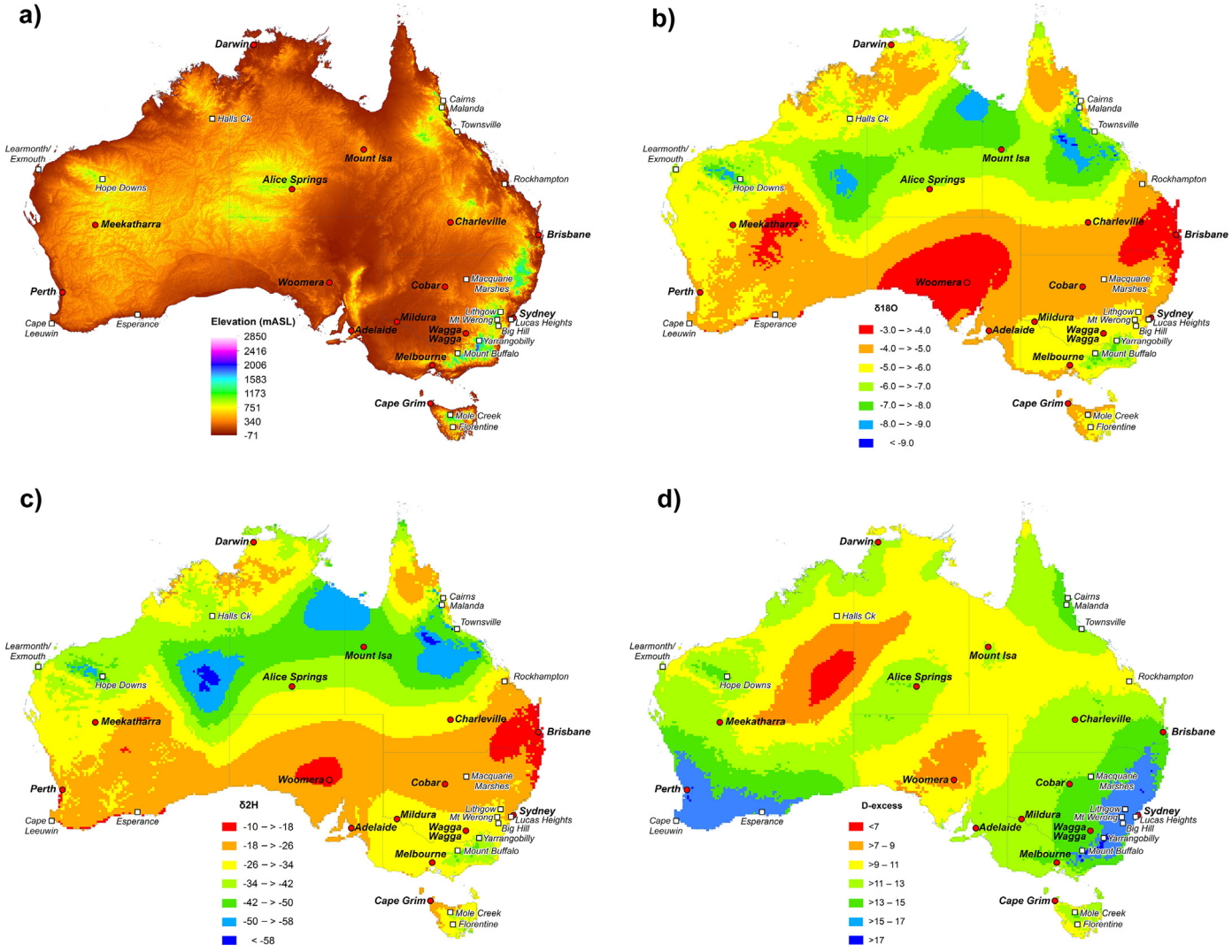

Fig. 6. a) Digital elevation model and location of all sites used in isoscape development. Annual isoscapes (‰) for b) $\delta^{18}O$; c) $\delta^{2}H$; and d) d_p. GNIP sites are shown as red circles and additional sites as white squares.

generating a regression without distance from the coast resulted in an r^2 of 0.99. If more parameters were to be resolved in the regression fit we found that this overfitting of the data presented some problems during the use of the regression model for prediction. The determined parameters of the regression fits are presented in Supplementary Table S5.

Once the equations for each region were determined, the Australian region was subdivided in to grid cells of 10′ and a value of the isotopic composition for each grid cell was estimated using the regression equations. To overcome a subjective choice of defining a boundary between the regions (for which a different regression fit was determined), a distance weighed procedure was used (similar to that used by Bowen and Revenaugh, 2003, for the interpolation of the error). Basically, the estimated isotopic value was a weighted sum from using each of the five equations with the local values of the predictor variables. The weight was the negative exponential of distance (in degrees) between the location of the grid cell and each of the measurement sites, i.e.

$$p_x = \frac{\sum_{i=1}^{n} y_i e^{-\left(D_i^x/B\right)}}{\sum_{i=1}^{n} e^{-\left(D_i^x/B\right)}} \tag{2}$$

where p_x is the predicted values of the isotopic composition in cell x, n is the number of observation sites, y_i is the regression equation associated with site i (but using the values for grid cell x for the predictor variables), D_i^x is the distance between the grid cell x and the measurement site i, and B is a smoothing parameter. The estimated isotopic value of grid cell x was then determined as the sum of p_x in Eq. (2) and an interpolated error term (err_x):

$$err_x = \frac{\sum_{i=1}^{n} err_i e^{-\left(D_i^x/B\right)}}{\sum_{i=1}^{n} e^{-\left(D_i^x/B\right)}} \tag{3}$$

where err_i is the difference between the measured value at site i and that estimated using Eq. (2). The value of B in Eqs. (2) and (3) was estimated by removing the measurement sites, one at a time and then minimising the difference between the estimated and measured values (resulting in a value of 1.45 for B). This was confirmed by a Moran's (1948) test where correlations between the errors and the spatial locations existed, with a p-value of 0.07 for errors in $\delta^{18}O$ and a p-value of 0.09 for errors in $\delta^{2}H$.

Once the isoscapes were developed a comparison was made between the estimated d using two methods; (1) using the measured d values and developing an isoscape of d and (2) using the isoscape derived values of $\delta^{18}O$ and $\delta^{2}H$ and using the relationship $d = \delta^{2}H -$

8δ^{18}O. The maximum difference between the *d* as calculated from the isoscape and the *d* as calculated from δ^{18}O and δ^{2}H was 0.01%.

As in Terzer et al. (2013), jackknifing (Wu, 1986) was used to determine the robustness of the model results. In this approach, all sites were removed one at a time and the values re-estimated over the Australian region. Then the mean and standard deviations of the estimates at each grid cell were determined. However, two approaches were implemented. In the first approach (regression jackknife), when a site was removed the regression models were re-determined; in the second approach (interpolation jackknife) the regression models remained as determined when all the sites were used but the interpolation was undertaken leaving the selected site out. The regression jackknife gives an indicator of the sensitivity of the regressions to outliers and the second to extrapolation only. In the context of the data used here the biggest issue was where the removal of a single site significantly reduced the range of a key variable in the regression e.g. for the "North", removal of Darwin results in a very small latitudinal range and removal of Malanda (Fig. 6; Cook et al., 2001) significantly reduces the elevation range; in both of these cases the resulting regression fits a smaller parameter range increasing the geographical areas requiring extrapolation of the regression. For this reason we believe that the regression jackknife is not the best indicator of the predictive ability of the isoscape, however it does highlight the areas where additional data is required to improve the regressions underpinning the isoscape.

The resulting annual isoscapes for δ^{18}O, δ^{2}H and d_p are shown in Fig. 6. Large standard deviations in either jackknife approach (Supplementary Fig. S3) indicate areas where the predictive strength of the isoscape are weakest, however, it is important to note that these are not errors or uncertainties, as these cannot be determined for locations where measured data is not available. The interpolation jackknife shows that the areas where the predictive strength of the isoscape are weakest are those where the most depleted isotopic composition is predicted in Fig. 6b and c along the Great Dividing Range in Central and North Queensland, and from the Gibson Desert west of Alice Springs through to the Gulf of Carpentaria. Whilst they are all subject to extreme events and monsoonal influences which render the predictions of the isoscape feasible, these are the areas which should be considered the highest priority for additional rainfall sampling.

There are significant spatial differences between this isoscape and RCWIP (Terzer et al., 2013) and OIPC (Bowen and Revenaugh, 2003; Bowen, 2018). Neither of the previous attempts reflect the depleted precipitation observed in the Pilbara region of NW Australia (Hope Downs) and the Gulf of Carpenteria (Mt Isa) which is largely due to tropical cyclones and the monsoon. In particular RCWIP predicts that the northern inland region will have extremely enriched precipitation, presumably because of the very low annual rainfall away from the coast, however, infrequent larger events actually dominate this zone leading to more depleted rainfall. RCWIP also predicts precipitation in the southern parts of Australia will be more depleted than this isoscape, whereas the predictions of OPIC (Bowen, 2018; Bowen and Revenaugh, 2003) are closer. Significant additional data for SE Australia in this paper enable a higher degree of confidence in the spatial distribution for this region in our isoscape than previously possible.

3.4. Precipitation and groundwater comparison

Groundwater studies rely on using the δ^{18}O and δ^{2}H of water to assess its origin and recharge processes in aquifers worldwide (e.g.: Wassenaar et al., 2009; West et al., 2014; Raidla et al., 2016). In high rainfall areas where groundwater is recharged rapidly, it typically retains the isotopic signature of rainfall. The isotopic composition of the groundwater will plot close to the MWL and is close to the mean precipitation weighted annual composition (Clark and Fritz, 1997), and may even reflect the seasonal isotopic signature of rainfall (Jasechko et al., 2014; Bryan et al., 2016). This recharge mechanism is seen along the SE and SW Australian coastal fringe, e.g. the Sydney region (Cendón et al., 2014b; Fig. 7a) where groundwater sits close to the LMWL, between the winter and summer weighted averages. However, the groundwater from the inland arid and semi-arid environments can reflect the episodic nature of rainfall events and/or the localised recharge of evaporatively enriched surface water that may not be derived from local precipitation. In these environments, the groundwater can be isotopically depleted relative to the annual mean rainfall, reflecting instead the mean precipitation weighted composition of rainfall events above some recharge threshold value (e.g. Harrington et al., 2002). In the Georgina Basin (Spencer, 2009; Fig. 7b) groundwater is more depleted than the weighted average rainfall and instead reflects the large rainfall events which are associated with cyclonic and monsoonal activity in the summer months, an effect seen broadly across the semi-arid northern inland (e.g. Cendón et al., 2010; Harrington et al., 2002; Dogramaci et al., 2012; Meredith et al., 2018). Groundwater can also be enriched and evaporated where recharge is driven by widescale flooding

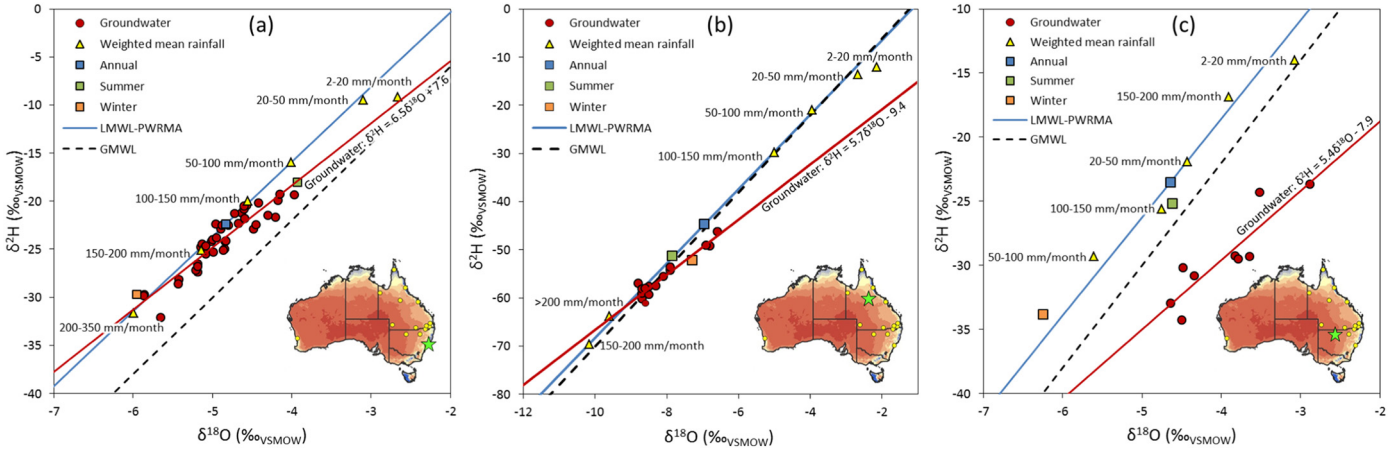

Fig. 7. Comparison between δ^{2}H and δ^{18}O values from shallow, relatively young (<50 years old) groundwater and the LMWL and precipitation amount-weighted mean compositions of different monthly rainfall amounts at three sites (represented by green stars). (a) Sydney rainfall and Hawkesbury Sandstone (Kulnura-Mangrove Mountain Aquifer, NSW) groundwater samples (Cendón et al., 2014b). Evaporation prior to recharge is limited and comparison with rainfall averages suggest that monthly rainfall >100 mm leads to recharge. (b) Mount Isa rainfall and Georgina Basin groundwater samples (Lawn Hill, Qld; Spencer, 2009). The groundwater samples plot close to or just to the right of the annual/summer LMWLs for Mount Isa, indicating some evaporation prior to recharge. The plot strongly suggests that recharge of groundwater occurs only after intense rainfall events of >150 mm/month. (c) Cobar rainfall and Darling River Basin (Glen Villa, NSW) groundwater samples (Meredith et al., 2015). Groundwater recharge occurs during flooding originating up to 800 km away.

originating hundreds or thousands of kilometres upstream (e.g. Meredith et al., 2015; Fig. 7c). Evaporative enrichment in the unsaturated zone during recharge is also well documented in arid and semi-arid regions and has been found to strongly influence the local groundwater isotopic composition (e.g. Barnes and Allison, 1988; Markowska et al., 2016).

One important application of the isoscape derived in this study is to support and guide the interpretation of $\delta^{18}O$ and $\delta^{2}H$ values in groundwater studies collected from rainfall isotope data-poor regions. Comparing the theoretical meteoric origin of groundwater, independent of the recharge mechanism, with short residence time groundwater samples, provides an opportunity to test the predictive capability of the isoscape as well as identifying regions of potential decoupling between precipitation and groundwater. Fourteen groundwater studies in northern and eastern Australia were selected for comparison with our precipitation isoscape (Fig. 1b; Supplementary Table S6). Most data are from Quaternary alluvial valleys (Baskaran et al., 2002; Cendón et al., 2010, 2014a; DSITIA, 2014; Duvert et al., 2015; Hankin and Cendón, 2014; Herczeg, 2004; Iverach et al., 2017; King et al., 2015; Martinez et al., 2017; Meredith et al., 2015; Please et al., 2000; Taylor et al., 2016; van der Ley, 2016); with the exception of Lawn Hill (karst system; Spencer, 2009), Atherton Tablelands (basalt plateau; Cook et al., 2001) and Kulnura-Mangrove Mountain (fractured sandstone Cendón et al., 2014b). Only samples with either quantifiable tritium concentrations, high radiocarbon (>80 pmc), and sourced from <100 m in depth have been incorporated in an effort to ensure groundwater was representative of modern recharge (<~100 yr).

Agreement between the isoscape and the groundwater isotope signature is very close for some sites but has significant scatter around the 1:1 line with an r^2 of 0.46 for $\delta^{2}H$ and 0.49 for $\delta^{18}O$. The underlying reasons for this scatter are best investigated by comparing the isoscape precipitation and measured groundwater d_p (Fig. 8). Here we see that in high rainfall locations, groundwater d_p is well predicted by the isoscape (falling on the 1:1 line) confirming that these sites receive direct rainfall recharge. Groundwater d_p becomes progressively lower than the isoscape d_p (dashed line in Fig. 8) as aridity and distance from the coast increases. This can be interpreted both in terms of the potential for evaporation *during* recharge, but also, more importantly in Australia, the distance from the headwaters of river systems and the potential for evaporation of surface water *prior to* recharge. In this dataset, a third factor is evident for inland groundwater expected to be closer to the dashed line, based on their geographical position: mixing of old groundwater, discharging from underlying Great Artesian Basin (GAB) formations into alluvial valleys (Iverach et al., 2017). The GAB groundwater component was probably recharged in distant areas closer to the coastline and eventually mixes with young locally-recharged and more evaporated water. The source of water in all these cases is the same – the Great Dividing Range, where precipitation is more depleted than seen further inland because of the higher altitude. The difference is whether groundwater recharges then follows a subsurface pathway to the sample location, or it is recharged locally following evaporation.

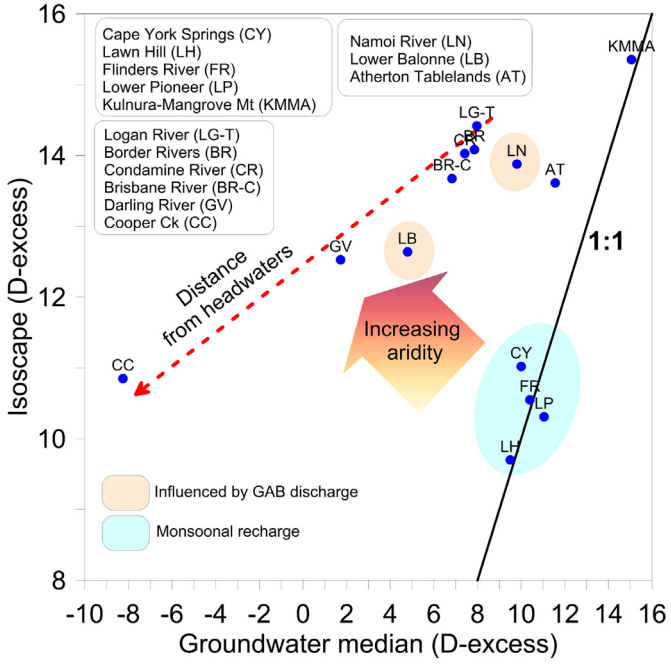

Fig. 8. Comparison between d_p predicted by the isoscape and that observed in modern groundwater.

The comparison of the isoscape and groundwater stable isotope records show the predictive capability of the isoscape, particularly along the eastern margin of the continent (Great Dividing Range) or in regions dominated by seasonal (local) recharge processes (e.g.: monsoon). The disconnect between the isoscape and groundwater reveals the increased aridity towards the centre of the continent with sites at ~700 km (GV) and 1100 km (CC) from the coast disconnected from local rainfall and relying on rainfall further upstream and flooding events to produce local groundwater recharge.

4. Conclusions

Australia, with an area of 7.7 million km^2 ranging in latitude 12.5 to 43°S and spanning 40° in longitude, is the lowest and flattest of all continents. The original Australian GNIP network (seven stations) has been more than doubled with the last 8–12 years of data in the 15 station network presented and interpreted in this paper.

Overall the interpretation supports the findings of Liu et al. (2010) for coastal areas, but adds far more to our understanding of inland Australia and many of the key water-resource limited areas such as the Murray-Darling Basin. Local meteoric water lines were developed for each site, as well as for the Australian continent. We recommend the use of precipitation weighted local meteoric water lines in any hydrological application of this dataset to better reflect the hydrological impact of rain. When the annual precipitation weighted values were used to generate an Australian meteoric water line, the line ($\delta^{2}H = 8.3\ \delta^{18}O + 14.1‰$) was close to that developed from the isoscape ($\delta^{2}H = 8.6\ \delta^{18}O + 14.4‰$).

A weak seasonal variation in the isotopic composition was evident with winter minimum and spring-summer maxima at the coastal temperate sites of Adelaide, Brisbane, Cape Grim, Melbourne and Sydney. Whereas, Alice Springs and the new inland sites (Charleville, Cobar, Mildura, Mt. Isa, Wagga Wagga, and Woomera) exhibit a spring maximum and lower values both in winter, and in summer when high rainfall events associated with tropical cyclones and the passage of the ITCZ are important. Precipitation amount was found to be a stronger driver of isotopic composition than temperature, particularly at the northern sites affected by tropical cyclones and the monsoon. Latitude, elevation and distance from the coast were found to be stronger drivers of spatial variability than temperature or rainfall amount, and the higher density of sites provides some opportunity to look at the effect of rainout and continentality across eastern Australia.

Annual isoscapes of $\delta^{2}H$, $\delta^{18}O$ and d_p developed using regional groupings rather than climate zones allowed us to take into account the varying importance of continentality due to either eastward or onshore movement of moisture and rainfall across the continent. Apart from doubling of spatial data points, in order to develop an isoscape other available short term rainfall data sets were used, either directly or as check of the predictive power of the isoscape. These additional datasets proved important in areas in the north of the continent affected by tropical cyclones and the monsoon, as well as ones representing high elevation areas in Australia.

Considering the importance of groundwater resources in the driest inhabited continent, precipitation records were compared to short residence-time groundwater data. Isotopic data from alluvial or fractured rock aquifers in the north and eastern coastal sites tend to be closely correlated with the local rainfall predicted by the isoscape. However, an increasing disconnect between local precipitation and groundwater is observed inland, highlighting the importance of flooding events to groundwater recharge. In both cases comparisons to groundwater highlight water stable isotope precipitation records as a tool for evaluating recharge and evaporation in local groundwater and surface water resources.

Data statement

GNIP data used for this paper will be made available through the Global Network of Isotopes in Precipitation database. The data and isoscape results have been published in an institutional data repository:

Precipitation isotope data for sites in Table 1 can be downloaded from: http://research-data.ansto.gov.au/collection/881

Gridded precipitation isoscape data can be downloaded from: http://research-data.ansto.gov.au/collection/880

Additional data and updates will be available at: http://www.ansto.gov.au/ozwin

Acknowledgements

The Australian GNIP network is supported by our long-standing partners, the Australian Bureau of Meteorology and the International Atomic Energy Agency. Much of the historical data was analysed by the Commonwealth Scientific and Industrial Research Organisation. John Gibson provided the much-appreciated impetus to expand the network in 2006. Our isoscape depended on data kindly provided by Greg Skrzypek (University of Western Australia), Steve Lewis (James Cook University), Niels Munksgaard (Charles Darwin University), Russell Crosbie (CSIRO), Pauline Treble and Alan Griffiths (ANSTO). Lastly we would like to acknowledge and thank all the ANSTO people who contributed to this work: Barbora Gallagher, Robert Chisari, Kellie-Anne Farrawell, Scott Allchin, Chris Dimovski, Charmaine Day and Jenny van Holst in the lab; Stuart Hankin for GIS support; and Pauline Treble for commenting on a draft of the paper. This research did not receive any grant from funding agencies in the public, commercial, or not-for-profit sectors.

Appendix A. Supplementary data

Supplementary data to this article can be found online at https://doi.org/10.1016/j.scitotenv.2018.07.082.

References

Adomako, D., Maloszewski, P., Stumpp, C., Osae, S., Akiti, T.T., 2010. Estimating groundwater recharge from water isotope (δ^2H, $\delta^{18}O$) depth profiles in the Densu River basin, Ghana. Hydrol. Sci. J. 55, 1405–1416.

Araguás-Araguás, L., Froehlich, K., Rozanski, K., 2000. Deuterium and oxygen-18 isotope composition of precipitation and atmospheric moisture. Hydrol. Process. 14, 1341–1355.9.

Baldini, L.M., McDermott, F., Baldini, J.U.L., Fischer, M.J., Mollhoff, M., 2010. An investigation of the controls on Irish precipitation $\delta^{18}O$ values on monthly and event timescales. Clim. Dyn. 35:977–993. https://doi.org/10.1007/s00382-010-0774-6.

Barnes, C.J., Allison, G.B., 1988. Tracing of water movement in the unsaturated zone using stable isotopes of hydrogen and oxygen. J. Hydrol. 100, 143–176.

Barras, V.J.L., Simmonds, I., 2008. Synoptic controls upon $\delta^{18}O$ in southern Tasmanian precipitation. Geophys. Res. Lett. 35, L02707. https://doi.org/10.1029/2007GL031835.

Barras, V., Simmonds, I., 2009. Observation and modelling of stable water isotopes as diagnostics of rainfall dynamics over southeastern Australia. J. Geophys. Res. 114, D23308. https://doi.org/10.1029/2009JD012132.

Baskaran, S., Budd, K.L., Larsen, R.M., Bauld, J., 2002. A groundwater quality assessment of the Lower Pioneer Catchment. Qld. Bureau of Rural Sciences, Canberra.

Bowen, G.J., 2018. The Online Isotopes in Precipitation Calculator, Version 3.1. http://www.waterisotopes.org.

Bowen, G.J., Revenaugh, J., 2003. Interpolating the isotopic composition of modern meteoric precipitation. Water Resour. Res. 39, 1299.

Bowen, G.J., Wilkinson, B., 2002. Spatial distribution of $\delta^{18}O$ in meteoric precipitation. Geology 30, 315–318.

Bowen, G.J., Wassenaar, L.I., Hobson, K.A., 2005. Global application of stable hydrogen and oxygen isotopes to wildlife forensics. Oecologia 143, 337–348.

Bryan, E., Meredith, K.T., Baker, A., Post, V.E.A., Andersen, M.S., 2016. Island groundwater resources, impacts of abstraction and a drying climate: Rottnest Island, Western Australia. J. Hydrol. 542, 704–718.

Callow, N., McGowan, H., Warren, L., Speirs, J., 2014. Drivers of precipitation stable oxygen isotope variability in an alpine setting, Snowy Mountains, Australia. J. Geophys. Res. Atmos. 119, 3016–3031.

Cartwright, I., Morgenstern, U., 2016. Contrasting transit times of water from peatlands and eucalypt forests in the Australian Alps determined by tritium: implications for vulnerability and the source of water in upland catchments. Hydrol. Earth Syst. Sci. 20 (12), 4757–4773.

Cartwright, I., Cendón, D., Currell, M., Meredith, K., 2017. A review of radioactive isotopes and other residence time tracers in understanding groundwater recharge: possibilities, challenges, and limitations. J. Hydrol. 555, 797–811.

Cendón, D.I., Larsen, J.R., Jones, B.G., Nanson, G.C., Rickleman, D., Hankin, S.I., Pueyo, J.J., Maroulis, J., 2010. Freshwater recharge into a shallow saline groundwater system, Cooper Creek floodplain, Queensland, Australia. J. Hydrol. 392, 150–163.

Cendón, D.I., Hankin, S., Kelly, B., Hollins, S., Martel, L., 2014a. Hydrogeochemistry and Isotopes in Groundwater From the Condamine Catchment Alluvial Aquifer System (SE-QLD)- Implications for Residence Times and Recharge. ANSTO/C-1395 Revision A (Prepared for the Cotton Research Development Corporation, 59 pp and Appendices).

Cendón, D.I., Hankin, S.I., Williams, J.P., Van der ley, M., Peterson, M., Hughes, C.E., Meredith, K., Graham, I.T., Hollins, S.E., Levchenko, V., Chisari, R., 2014b. Groundwater residence time in a dissected and weathered sandstone plateau: Kulnura–Mangrove Mountain aquifer, NSW, Australia. Aust. J. Earth Sci. 62:123–141. https://doi.org/10.1080/08120099.2014.893628.

Clark, I.D., Fritz, P., 1997. Environmental Isotopes in Hydrogeology. Lewis Publishers, New York, p. 328.

Cook, P.G., Herczeg, A.L., McEwan, K.L., 2001. Groundwater Recharge and Stream Baseflow: Atherton Tablelands, Queensland. CSIRO Land and Water Technical Report 08/01, April 2001.

Craig, H., 1961. Isotopic variation in meteoric waters. Science 133, 1702–1703.

Crawford, J., Hughes, C.E., Parkes, S.D., 2013. Is the isotopic composition of event based precipitation driven by moisture source or synoptic scale weather in the Sydney Basin, Australia? J. Hydrol. 207, 213–226.

Crawford, J., Hughes, C.E., Lykoudis, S., 2014. Alternative least squares method for determining the meteoric water line, demonstrated using GNIP data. J. Hydrol. 519, 2331–2340.

Crawford, J., Hollins, S.E., Meredith, K.T., Hughes, C.E., 2017. Precipitation stable isotope variability and sub-cloud evaporation processes in a semi-arid region. Hydrol. Process. 31, 20–34.

Crosbie, R., Morrow, D., Cresswell, R., Leaney, F., Lamontagne, S., Lefournour, M., 2012. New insights to the chemical and isotopic composition of rainfall across Australia. Water for a Healthy Country Flagship Report Report EP125581 ISSN: 1835-095X. 76pp. https://doi.org/10.5072/83/5849a0d6c685a.

Dansgaard, W., 1964. Stable isotopes in precipitation. Tellus 16, 436–468.

Dogramaci, S., Skrzypek, G., Dodson, W., Grierson, P.F., 2012. Stable isotope and hydrochemical evolution of groundwater in the semi-arid Hamersley Basin of subtropical northwest Australia. J. Hydrol. 475, 281–293.

Draxler, R.R., Rolph, G.D., 2003. Hybrid Single-Particle Lagrangian Integrated Trajectory (HYSPLIT). model. http://www.arl.noaa.gov/ready/hysplit4.html>.

DSITIA, 2014. Western Cape York Groundwater Study 2. Groundwater Dependent Ecosystems Investigation Supporting the Assessment of Groundwater Sustainability in the Great Artesian Basin of Cape York. Dept Science, Information Technology, Innovation and the Arts, Brisbane (167 pp).

Duvert, C., Raiber, M., Owen, D.D.R., Cendón, D.I., Batiot-Guilhe, C., Cox, M.E., 2015. Hydrochemical processes in a shallow coal seam gas aquifer and its overlying stream–alluvial system: implications for recharge and inter-aquifer connectivity. Appl. Geochem. 61, 146–159.

Edirisinghe, E.A.N.V., Pitawala, H.M.T.G.A., Dharmagunawardhane, H.A., Wijayawardane, R.L., 2017. Spatial and temporal variation in the stable isotope composition ($\delta^{18}O$ and δ^2H) of rain across the tropical island of Sri Lanka. Isot. Environ. Health Stud. 1–18.

Feng, X., Faiia, A.M., Posmentier, E.S., 2009. Seasonality of isotopes in precipitation: a global perspective. J. Geophys. Res. 114, D08116. https://doi.org/10.1029/2008JD11279.

Froehlich, K., Gibson, J.J., Aggarwal, P.K., 2002. Deuterium excess in precipitation and its climatological significance. Proc. Study of Environmental Change Using Isotope Techniques, IAEA, Vienna, IAEA-CSP-13/P, pp. 54–66.

Gedzelman, S., Lawrence, J., Gamache, J., Black, M., Hindman, E., Black, R., Dunion, J., Willoughby, H., Zhang, X., 2003. Probing hurricanes with stable isotopes of rain and water vapor. Mon. Weather Rev. 131, 1112–1127.

Goede, A., Green, D.C., Harmon, R.S., 1982. Isotopic composition of precipitation, cave drips and actively forming speleothems at three Tasmanian cave sites. Helictite 20, 17–28.

Goede, A., Green, D.C., Harmon, R.S., 1986. Late Pleistocene palaeotemperature record from a Tasmanian speleothem. Aust. J. Earth Sci. 33, 333–342.

Goede, A., Veer, H.H., Ayliffe, L.K., 1990. Late Quaternary palaeotemperature records for two Tasmanian speleothems. Aust. J. Earth Sci. 37, 267–278.

Guan, H., Simmons, C.T., Love, A.J., 2009. Orographic controls on rain water isotope distribution in the Mount Lofty Ranges of South Australia. J. Hydrol. 374, 255–264.

Guan, H., Zhang, X., Skrzypek, G., Sun, Z., Xu, X., 2013. Deuterium excess variations of rainfall events in a coastal area of South Australia and its relationship with synoptic weather systems and atmospheric moisture sources. J. Geophys. Res.-Atmos. 118: 1–16. https://doi.org/10.1002/jgrd.50137.

Hankin, S., Cendón, D.I., 2014. Measurement and Preliminary Interpretation of Isotopes in Groundwater at Talwood, QLD. ANSTO/C-1434 (34 pp).

Harrington, G.A., Herczeg, A.L., Cook, P.G., 2002. Spatial and temporal variability of ground water recharge in Central Australia: a tracer approach. Ground Water 40, 518–528.

Harvey, F.E., 2001. Use of NADP archive samples to determine the isotope composition of precipitation: characterizing the meteoric input function for use in ground water studies. Ground Water 39 (3), 380–390.

Harvey, F.E., Welker, J.M., 2000. Stable isotopic composition of precipitation in the semi-arid north-central portion of the US Great Plains. J. Hydrol. 238, 90–109.

Herczeg, A.L., 2004. Groundwater ages, sources of salt and recharge mechanisms in the Lower Balonne area, southern Queensland, Australia: isotope and geochemical data. CRC LEME Open File Report 164, October 2004.

Hughes, C.E., Crawford, J., 2012. A new precipitation weighted method for determining the meteoric water line for hydrological applications demonstrated using Australian and global GNIP data. J. Hydrol. 464–465, 42–55.

Hughes, C.E., Crawford, J., 2013. Spatial and temporal variation in precipitation isotopes in the Sydney Basin, Australia. J. Hydrol. 489, 42–55.

IAEA/WMO, 2017. Global Network of Isotopes in Precipitation. The GNIP Database. Accessible at:. http://www.iaea.org/water.

International Atomic Energy Agency, 1992. Statistical Treatment of Data on Environmental Isotopes in Precipitation: Technical Reports Series No. 331. International Atomic Energy Agency, Vienna, p. 781.

International Atomic Energy Agency, 2014. RCWIP (Regionalized Cluster-Based Water Isotope Prediction) Model – Gridded Precipitation $\delta^{18}O|\delta^{2}H|$ $\delta^{18}O$ and $\delta^{2}H$ Isoscape Data. International Atomic Energy Agency, Vienna, Austria 2014, available at. http://www.iaea.org/water (downloaded at 14/1/2014).

Iverach, C.P., Cendón, D.I., Meredith, K.T., Wilcken, K.M., Hankin, S.I., Andersen, M.S., Kelly, B.F.J., 2017. A multi-tracer approach to constraining artesian groundwater discharge into an alluvial aquifer. Hydrol. Earth Syst. Sci. Discuss. 1–40 2017.

Jasechko, S., Birks, S.J., Gleeson, T., Wada, Y., Fawcett, P.J., Sharp, Z.D., McDonnell, J.J., Welker, J.M., 2014. The pronounced seasonality of global groundwater recharge. Water Resour. Res. 50 (11), 8845–8867.

Kalbus, E., Reinstrof, F., Schirmer, M., 2006. Measuring methods for groundwater - surface water interactions: a review. Hydrol. Earth Syst. Sci. Discuss. Eur. Geosci. Union 10 (6), 873–887.

King, A.C., Raiber, M., Cendón, D.I., Cox, M.E., Hollins, S.E., 2015. Identifying flood recharge and inter-aquifer connectivity using multiple isotopes in subtropical Australia. Hydrol. Earth Syst. Sci. 19, 2315–2335.

Kumar, B., Rai, S.P., Kumar, U.S., Verma, S.K., Grag, P., Kumar, S.V.V., Jaiswal, R., Purendra, B. K., Kumar, S.R., Pande, N.G., 2010. Isotopic characteristics of Indian precipitation. Water Resour. Res. 46, W12548. https://doi.org/10.1029/2009WR008532.

Lawrence, J.R., Gedzelman, S.D., 1996. Low stable isotope ratios of tropical cyclone rains. Geophys. Res. Lett. 23, 527–530.

Liotta, M., Favara, R., Valenza, M., 2006. Isotopic composition of the precipitations in the central Mediterranean: origin marks and orographic precipitation effects. J. Geophys. Res.-Atmos. 111 (D19). https://doi.org/10.1029/2005jd006818.

Liu, J., Fu, G., Song, X., Charles, S.P., Zang, Y., Han, D., Wang, S., 2010. Stable isotopic compositions in Australian precipitation. J. Geophys. Res. 115, D23307. https://doi.org/10.1029/2010JD014403.

Lykoudis, S.P., Argiriou, A.A., 2007. Gridded data set of the stable isotopic composition of precipitation over the eastern and central Mediterranean. J. Geophys. Res. Atmos. 112, D18107.

Markowska, M., Baker, A., Andersen, M.S., Jex, C.N., Cuthbert, M.O., Rau, G.C., Graham, P. W., Rutlidge, H., Mariethoz, G., Marjo, C.E., Treble, P.C., Edwards, N., 2016. Semi-arid zone caves: evaporation and hydrological controls on $\delta^{18}O$ drip water composition and implications for speleothem paleoclimate reconstructions. Quat. Sci. Rev. 131, 285–301.

Martinez, J.L., Raiber, M., Cendón, D.I., 2017. Using 3D geological modelling and geochemical mixing models to characterise alluvial aquifer recharge sources in the upper Condamine River catchment, Queensland, Australia. Sci. Total Environ. 574, 1–18.

Matsui, E., Salati, E., Ribeiro, M.N.G., Reis, C.D., Tancredi, A.C.S.N.F., Gat, J.R., 1983. Precipitation in the Central Amazon basin: the isotopic composition of rain and atmospheric moisture at Belém and Manaus. Acta Amazon. 13 (2), 307–369.

McDermott, F., 2004. Paleo-climate reconstruction from stable isotope variations in speleothems: a review. Quat. Sci. Rev. 23, 901–918.

Meredith, K.T., Hollins, S.E., Hughes, C.E., Cendón, D.I., Chisari, R., Griffiths, A., Crawford, J., 2015. Evaporation and concentration gradients created by episodic river recharge in a dryland aquifer: insights from Cl, $\delta^{18}O$, $\delta^{2}H$ and ^{3}H. J. Hydrol. 529:1070–1078. https://doi.org/10.1016/j.jhydrol.2015.09.025.

Meredith, K.T., Han, L.F., Cendón, D.I., Crawford, J., Hankin, S., Peterson, M., Hollins, S.E., 2018. Evolution of dissolved inorganic carbon in groundwater recharged by cyclones and groundwater age estimations using the ^{14}C statistical approach. Geochim. Cosmochim. Acta 220 (Supplement C), 483–498.

Moran, P.A.P., 1948. The interpretation of statistical maps. J. R. Stat. Soc. Ser. B (Methodol.) 10 (2), 243–251.

Munksgaard, N.C., Zwart, C., 2017. Pers. comm. 4/4/2017 Data From IAEA Coordinated Research Project (CRP) F31004 "Stable Isotopes in Precipitation and Paleoclimatic Archives in Tropical Areas to Improve Regional Hydrological and Climatic Impact Models.

Munksgaard, N.C., Zwart, C., Kurita, N., Bass, A., Nott, J., Bird, M.I., 2015. Stable isotope anatomy of tropical cyclone Ita, North-Eastern Australia, April 2014. PLoS One https://doi.org/10.1371/journal.pone.0119728.

Pfahl, S., Sodemann, H., 2014. What controls deuterium excess in global precipitation? Clim. Past 10, 771–781.

Please, F.M., Watkins, K.L., Cresswell, R.G., Bauld, J., 2000. A Groundwater Quality Assessment of the Alluvial Aquifers in the Border Rivers Catchment (Qld/NSW). Bureau of Rural Sciences, Canberra, Australia.

Raidla, V., Kern, Z., Pärn, J., Babre, A., Erg, K., Ivask, J., Kalvāns, A., Kohán, B., Lelgus, M., Martma, T., Mokrik, R., 2016. A $\delta^{18}O$ isoscape for the shallow groundwater in the Baltic Artesian Basin. J. Hydrol. 542, 254–267.

Risbey, J.S., Pook, M.J., McIntosh, P.C., 2009. On the remote drivers of rainfall variability in Australia. Mon. Weather Rev. 137, 3233–3253.

Risi, C., Bony, S., Vimeux, F., 2008. Influence of convective processes on the isotopic composition ($\delta^{18}O$ and δD) of precipitation and water vapour in the tropics: 2. Physical interpretation of the amount effect. J. Geophys. Res. 113, D19306. https://doi.org/10.1029/2008JD009943.

Rozanski, K., Araguás-Araguás, L., Gonfiantini, R., 1993. Isotopic patterns in modern precipitation. In: Swart, P.K., et al. (Eds.), Climate Change in Continental Isotopic Records. Geophys. Monogr. Ser. vol. 78. AGU, Washington, DC, pp. 1–36.

Scholl, M.A., Shanley, J.B., Zegarra, J.P., Coplen, T.B., 2009. The stable isotope amount effect: new insights from NEXRAD echo tops, Luquillo Mountains, Puerto Rico. Water Resour. Res. 45, W12407. https://doi.org/10.1029/2008WR007515.

Skrzypek, G., Mydlowski, A., Dogramaci, S., Hedley, P., Gibson, J., Grierson, P.F., 2015. Estimation of evaporative loss based on the stable isotope composition of water using hydrocalculator. J. Hydrol. 523, 781–789.

Skrzypek, G., Dogramaci, S., Rouillard, A., Grierson, P.F., 2018. Unique isotope signature of large cyclonic events as a tracer of ecohydrologic processes in the arid subtropics, NW Australia. J. Hydrol. (in preparation).

Spencer, J.J., 2009. The Surface and Ground Waters of the Lawn Hill Region, Northwest Queensland. UNSW (Unpublished Honours Thesis, 97 pp).

Stern, H., de Hoedt, G., Ernst, J., 2000. Objective classification of Australian climates. Aust. Meteorol. Mag. 49, 87–96.

Sturman, A., Tapper, N., 2006. The Weather and Climate of Australia and New Zealand. Oxford University Press.

Tadros, C.V., Treble, P.C., Baker, A., Fairchild, I., Hankin, S., Roach, R., Markowska, M., McDonald, J., 2016. ENSO – cave dripwater hydrochemical relationship: a 7-year dataset from SE Australia. Hydrol. Earth Syst. Sci. 20, 4625–4640.

Taylor, A.R., Smith, S.D., Lamontagne, S., Suckow, A., 2016. Characterisation of Shallow Alluvial Groundwater Resources Near Hughenden, Flinders Catchment, Queensland. A Report to the Queensland Government Dept of Agriculture and Fisheries and the Flinders Shire Council. CSIRO Report EP163793 (46 pp).

Terzer, S., Wassenaar, L.I., Araguás-Araguás, L.J., Aggarwal, P.K., 2013. Global isoscapes for $\delta^{18}O$ and $\delta^{2}H$ in precipitation: improved prediction using regionalized climatic regression models. Hydrol. Earth Syst. Sci. 17, 4713–4728.

Treble, P.C., Budd, W.F., Hope, P.K., Rustomji, P.K., 2005a. Synoptic-scale climate patterns associated with rainfall $\delta^{18}O$ in southern Australia. J. Hydrol. 302, 270–282.

Treble, P.C., Chappell, J., Gagan, M.K., McKeegan, K.D., Harrison, T.M., 2005b. In situ measurement of seasonal $\delta^{18}O$ variations and analysis of isotopic trends in a modern speleothem from southwest Australia. Earth Planet. Sci. Lett. 233 (1), 17–32.

Treble, P.C., Bradley, C., Wood, A., Baker, A., Jex, C.N., Fairchild, I.J., Gaga, M.K., Cowley, J., Azcurra, C., 2013. An isotopic study of flow paths and storage in Quaternary calcarenite, SW Australia: implications for speleothem paleoclimate records. Quat. Sci. Rev. 64, 90–103.

Vachon, R.W., Welker, J.M., White, W.C., Vaughn, B.H., 2010. Moisture source temperatures and precipitation $\delta^{18}O$-temperature relationships across the United States. Water Resour. Res. 46, W07523. https://doi.org/10.1029/2009WR008558.

van der Ley, M., 2016. Hydrogeochemistry, Residence Times, and Flow Processes of Ground and Surface Waters in the Lawn Hill Region, Northwest Queensland, Australia. UNSW (Unpublished PhD Thesis, 368 pp).

Wassenaar, L.I., Van Wilgenburg, S.L., Larson, K., Hobson, K.A., 2009. A groundwater isoscape (δD, $\delta^{18}O$) for Mexico. J. Geochem. Explor. 102 (3), 123–136.

West, A.G., February, E.C., Bowen, G.J., 2014. Spatial analysis of hydrogen and oxygen stable isotopes ("isoscapes") in ground water and tap water across South Africa. J. Geochem. Explor. 145, 213–222.

Wu, C.F.J., 1986. Jackknife, bootstrap and other resampling methods in regression analysis. Ann. Stat. 14, 1261–1295.

Zwart, C., Munksgaard, N.C., Kurita, N., Bird, M.I., 2016. Stable isotopic signature of Australian monsoon controlled by regional convection. Quat. Sci. Rev. 151, 228–235.